Representation of Eddies in Primitive Equation Models by a PV Flux

RICHARD WARDLE

MIT/WHOI Joint Program, Massachusetts Institute of Technology, Cambridge, Massachusetts

JOHN MARSHALL

Program in Atmospheres, Oceans and Climate, Massachusetts Institute of Technology, Cambridge, Massachusetts

(Manuscript received 2 September 1998, in final form 12 November 1999)

ABSTRACT

The parametric representation of buoyancy and momentum transport by baroclinic eddies in a primitive equation ''β plane'' channel is studied through a transformation of the governing equations. Adoption of the ''transformed Eulerian mean'' and the assumption that the eddies (but not the mean flow) are quasigeostrophic in nature leads to 1) the eddies being represented symbolically by one term, an eddy potential vorticity flux, rendering a representation that incorporates both eddy momentum and eddy buoyancy fluxes, and 2) the advecting velocities being those of the residual mean circulation. A closure is employed for the eddy potential vorticity flux that directs it down the mean potential vorticity gradient. Care is taken to ensure that the resulting force does not generate any net momentum in the channel but only acts to redistribute it.

The approach is investigated by comparing a zonally averaged parameterized model with a three-dimensional eddy-resolving calculation of flow in a stress-driven channel. The stress at the upper surface is communicated down the water column to the bottom by eddy form drag. Moreover, lateral eddy momentum fluxes act to strengthen and sharpen the mean flow, transporting eastward momentum from the flanks to the center of the jet, up its large-scale gradient. Both vertical momentum transfer and lateral, upgradient momentum transfer by eddies, is captured in the parameterized model.

Finally, advantages of the parametric approach are demonstrated in two further contexts: 1) the spindown of a baroclinic zone and 2) the maintenance of surface winds by eddy momentum flux in the atmosphere.

1. Introduction

Representation of eddies in ocean models remains one of the outstanding computational and intellectual challenges in ocean modeling. To resolve the eddy field explicitly in models demands either that we study regional ocean circulation or that we embark on global eddy-resolving numerical calculations, which tax even the biggest and fastest computers available—see, for example, Semtner and Chervin (1992). In climate studies the most appealing way forward is to parameterize, rather than resolve, transfers of heat, momentum, and vorticity on the eddy scale. In quasigeostrophic models a framework is strongly suggested by the attendant potential vorticity (PV) theorem. The heat and momentum aspects of the eddy-transfer process can then be naturally combined by phrasing them in terms of PV transport—see, for example, Marshall (1981). Eddy closure, although still thwart with difficulties, is then at its most transparent. But the ocean is not quasigeostrophic. For example, it is inappropriate to linearize the thermodynamic equation about a constant reference stability profile which, in quasigeostrophic theory, cannot be allowed to vary in the horizontal. How, then, can we proceed in more complete models?

A potential vorticity theorem exists for the hydrostatic primitive equations (HPE), the starting point of most ocean models. But, unlike in quasigeostrophic models, the prognostic variable is not potential vorticity.[1] In the HPEs, momentum and temperature are stepped forward separately and the effect of the eddies (eddy momentum and heat flux divergences) appear as ''forcing terms'' on the rhs and are parameterized separately. We argue here that this separation of the heat and vorticity transporting properties of eddies—a separation dictated largely by algorithmic rather than physical considerations—significantly compli-

Corresponding author address: Richard Wardle, Department of Geophysical Sciences, University of Chicago, Chicago, IL 60637.
E-mail: rmwardle@geosci.uchicago.edu

[1] Some additional balance assumptions could perhaps be made to invert the PV for the primitive variables, but only at the expense of major complications in the treatment of the lateral boundaries, and the loss of gravity wave dynamics.

cates the parameterization problem and, if possible, should be avoided.

A way forward is provided if the full HPEs are ''transformed,'' guided by the formalism of the ''transformed Eulerian mean'' (TEM) of Andrews and McIntyre (1976). In the zonal average, and if the eddies are assumed to obey quasigeostrophic scaling and dynamics, their effect appears as a single term—an eddy PV flux—driving the momentum equation. Importantly, however, in the approach advocated here the lhs of the equations are retained in their full primitive equation form. Parameterization can then focus on the closure of the eddy PV flux that encapsulates both buoyancy and vorticity transporting properties of the eddy field.

Similar approaches have been outlined in Tung (1986), Lee and Leach (1996), and Greatbatch (1998), all of whom parameterize the eddies by means of a PV flux appearing in the averaged momentum equations. However, there are important differences between the present study and the aforementioned ones. First, we focus on the inclusion of eddy relative vorticity fluxes and, to facilitate this, simplify the eddy PV flux by adopting quasigeostrophic scaling for the eddies. Second, we remain in height coordinates. Third, and most importantly, we implement our scheme and directly compare it to the results of eddy-resolving primitive equation calculations.

We close for the eddies assuming a flux gradient relationship for potential vorticity and are able to represent cases in which momentum is transferred up its mean gradient, thus sharpening the large-scale jet. If the relative vorticity flux in the quasigeostrophic PV (QGPV) eddy flux is vanishingly small, then our scheme has a very similar form to that of Gent and McWilliams (1990) in the zonal average, although our PV perspective leads to a different implementation. In this paper we focus on the zonal-average problem because it is the simplest context in which to explore how to proceed. However, the approach set out here can also be applied in three dimensions (albeit if additional assumptions are made). That study will be reported later.

In section 2 we briefly review the theoretical background of the transformed Eulerian mean. The relationship between this approach and the parameterization of Gent and McWilliams (1990) is discussed. In section 3 we present our closure assumption, which asserts that the eddy potential vorticity flux is directed down the large-scale gradient of PV. To ensure that the parameterized eddies do not lead to erroneous sources or sinks of momentum, the form of the transfer coefficients are chosen to satisfy a zonal momentum constraint. Section 4 presents and discusses the parameterization approach in a stress-driven channel and compares the parameterized model to an eddy-resolving calculation. In section 5 we illustrate our approach through two further examples: the spindown of a baroclinic zone and the atmospheric ''surface wind'' problem.

2. Zonal average theory

a. The transformed Eulerian mean

The Eulerian mean zonally-averaged hydrostatic, primitive equations for Boussinesq flow, subject to forces $\mathbf{F} = (F^x, F^y)$, and source/sinks of buoyancy G, are

$$\overline{u}_t + \overline{v}\,\overline{u}_y + \overline{w}\,\overline{u}_z - f\overline{v} = \overline{F}^x - \boldsymbol{\nabla}\cdot\overline{(\mathbf{u}'u')} \quad (1a)$$

$$\overline{v}_t + \overline{v}\,\overline{v}_y + \overline{w}\,\overline{v}_z + f\overline{u} + \frac{1}{\rho_o}\overline{p}_y = \overline{F}^y - \boldsymbol{\nabla}\cdot\overline{(\mathbf{u}'v')} \quad (1b)$$

$$\overline{b} + \frac{1}{\rho_o}\overline{p}_z = 0 \quad (1c)$$

$$\overline{b}_t + \overline{v}\,\overline{b}_y + \overline{w}\,\overline{b}_z = \overline{G} - \boldsymbol{\nabla}\cdot\overline{(\mathbf{u}'b')} \quad (1d)$$

$$\overline{v}_y + \overline{w}_z = 0, \quad (1e)$$

where the zonal mean of a variable has been denoted by an overbar and the perturbation or eddy part has been denoted by a prime: $a(x, y, z, t) = \overline{a}(y, z, t) + a'(x, y, z, t)$. Further, in the zonal mean, gradients in the zonal direction vanish.

The effect of eddies appears as the divergence of the Reynolds stresses in the momentum equations and the divergence of the eddy buoyancy flux in the buoyancy equation. This separation of the momentum (vorticity) and buoyancy transporting properties of the eddy field has led to them being treated separately in models. For example, Reynolds stresses are almost universally represented as a Fickian process, $\boldsymbol{\nabla}\cdot\overline{(\mathbf{u}'u')} = -K\nabla^2 u$, in large-scale ocean models, even though it is known that geostrophic eddies can, and often do, ''unmix'' momentum—see Starr (1948). Indeed, because momentum is not conserved following the motion (it is constantly being changed by pressure gradient forces), there is no physical basis for using mixing length arguments for momentum and for adopting a Fickian-like closure.

A logical way forward is to transform the above equations so that the effect of the eddies on the large-scale appears as an eddy flux of a quasi-conserved and, hence, more transferable quantity, such as potential vorticity. This can be done by adopting the formalism of the transformed Eulerian mean. Following Andrews et al. (1987, section 3), let us ''transform'' the governing equations by introducing a ''residual mean meridional circulation''; thus

$$\overline{v}^* = \overline{v} - \left(\frac{\overline{v'b'}}{N^2}\right)_z, \quad (2a)$$

$$\overline{w}^* = \overline{w} + \left(\frac{\overline{v'b'}}{N^2}\right)_y, \quad (2b)$$

where the asterisks refer to a transformed velocity,[2] which we insist is nondivergent:

$$\overline{v}^*_y + \overline{w}^*_z = 0. \tag{3}$$

In Eq. (2) $N^2 \equiv \overline{b}^{xy}_z\,(z, t)$ is the horizontal mean of the buoyancy frequency and is independent of horizontal position. Substituting Eq. (2a,b) into (1a–e) and assuming that the eddies obey quasigeostrophic scaling, we obtain [details are given in Andrews et al (1987, section 3)]

$$\overline{u}_t + \overline{v}^*\overline{u}_y + \overline{w}^*\overline{u}_z - f\overline{v}^* = \overline{F}^x + \overline{v'q'} \tag{4a}$$

$$\overline{v}^*_t + \overline{v}^*\overline{v}^*_y + \overline{w}^*\overline{v}^*_z + f\overline{u} + \frac{1}{\rho_o}\overline{p}_y = \overline{F}^y \tag{4b}$$

$$\overline{b} + \frac{1}{\rho_o}\overline{p}_z = 0 \tag{4c}$$

$$\overline{b}_t + \overline{v}^*\overline{b}_y + \overline{w}^*\overline{b}_z = \overline{G} \tag{4d}$$

$$\overline{v}^*_y + \overline{w}^*_z = 0, \tag{4e}$$

where $\overline{v'q'}$ is the meridional eddy flux of quasigeostrophic potential vorticity, given by

$$\overline{v'q'} = -\overline{(u'v')}_y + f_o\left(\frac{\overline{(v'b')}}{N^2}\right)_z, \tag{5}$$

and f_o is a constant, middle-latitude value of the Coriolis parameter.

It should be emphasized here that we only adopt quasigeostrophic scaling *for the eddies,* thus rendering a simple form for the rhs of (4a) and (4b), but retain the full primitive equation form on the left, albeit with some reinterpretation of the terms.

There are five equations, Eq. (4a–e), and six unknowns: $\overline{u}$, $\overline{v}^*$, $\overline{w}^*$, $\overline{b}$, $\overline{p}$, and $\overline{v'q'}$. If the eddy flux $\overline{v'q'}$ can be expressed in terms of variables on the lhs of Eq. (4), then a closed set of prognostic equations for the zonal mean flow are obtained in which the eddies appear as a single body force in the zonal momentum equation.

In the developments that follow we will exploit the well-known relationship between $\overline{v'q'}$ and the Eliassen–Palm (E–P) flux (Eliassen and Palm 1961):

$$\overline{v'q'} = \nabla \cdot \mathbf{E}, \tag{6}$$

where

$$\mathbf{E} = \begin{pmatrix} E^y \\ E^z \end{pmatrix} = \begin{pmatrix} -\overline{(u'v')} \\ f_o\left(\dfrac{\overline{v'b'}}{N^2}\right) \end{pmatrix}. \tag{7}$$

The E–P flux is useful when thinking about the role of boundaries, particularly when used in conjunction with the ''potential vorticity sheets'' introduced by Bretherton (1966). Because PV sheets play an important role in our subsequent development, we discuss them briefly here. Drawing on insights from potential theory, Bretherton, again working within the confines of quasigeostrophic theory, recognized that boundary temperature (buoyancy) distributions are mathematically equivalent to concentrated sheets of quasigeostrophic potential vorticity just interior to the boundaries if those boundaries are then assumed to be isentropic (at constant buoyancy; $b' = 0$). Thus, if the vertical component of **E** (that associated with eddy buoyancy flux) is finite at an infinitesimal distance from the boundary, it is zero on the boundary itself in the presence of the PV sheet. This leads to a concentrated sheet of $\nabla \cdot \mathbf{E}$ representing PV fluxes associated with boundary buoyancy distributions.

In the presence of PV sheets there is an important and very useful integral constraint on the Eliassen–Palm flux divergence and the PV flux:

$$\int_{\text{Volume}} \nabla \cdot \mathbf{E}\, dV = \int_{\text{Volume}} \overline{v'q'}\, dV = 0, \tag{8}$$

where the eddy momentum flux at lateral boundaries is assumed to vanish and the upper and lower boundaries are isentropic. This can be seen directly from (5) since $v' = 0$ at the meridional walls and $b' = 0$ at the upper and lower boundaries. Thus, inspecting (4a) and (8), the eddies can provide no net force on the zonal mean flow and act only to redistribute zonal momentum. This momentum constraint will be exploited in section 3, to guide our choice of the spatial form of our eddy transfer coefficient.

b. Transformed Eulerian mean in the limit of vanishing relative vorticity flux

It is notable that in the transformed equations, eddy buoyancy flux divergence terms do not appear on the rhs of Eqs. (4a–e). This fact lies at the heart of the success of the parameterization of Gent and McWilliams (1990, hereafter GM). There, the eddy flux terms are related to an advective flux rather than to a diffusive process. In so doing, the diffusive nature of height-coordinate ocean models, which had compromised them since their inception, was in large part removed. In TEM the adiabatic nature of the eddy transfer process is automatically guaranteed because (and in contrast to GM) the eddy terms appear in the momentum, rather than the tracer equations. Thus the advecting velocities are changed by the introduction of an appropriate body

[2] In the oceanographic literature the difference between $\overline{v}^*$ and $\overline{v}$, in Eq. (2), is sometimes called an ''eddy-induced velocity,'' which, somewhat misleadingly, implies that the flow can be separated in to two parts: one of which is independent of the eddy disturbances and one that is the sole result of them. Instead we prefer to use the term ''residual mean velocities'' to describe $\overline{v}^*$, a nomenclature commonly used in meteorology.

force in the momentum equation rather than explicitly in the tracer equation. What is more, the vorticity and buoyancy transferring properties of the eddies are handled together and expressed in terms of the eddy transfer of a potential vorticity, which is more conserved than either vorticity or buoyancy alone.

If relative vorticity fluxes are neglected, then the eddy meridional flux of potential vorticity given by Eq. (5) reduces to (see the appendix)

$$\overline{v'q'} = f_o\left(\frac{\overline{(v'b')}}{N^2}\right)_z. \tag{9}$$

If the eddy buoyancy flux is related to the mean buoyancy gradient, thus

$$\overline{v'b'} = -K_b\overline{b}_y, \tag{10}$$

where K_b is an eddy transfer coefficient for buoyancy; then using the thermal wind equation, Eq. (9) becomes

$$\overline{v'q'} = \left(\frac{K_b f_o^2}{N^2}\overline{u}_z\right)_z, \tag{11}$$

where $\overline{u}_z$ is the vertical shear of the geostropic velocity. Using Eq. (11) the transformed zonal momentum equation can then be written:

$$\overline{u}_t + \overline{v}^*\overline{u}_y + \overline{w}^*\overline{u}_z - f\overline{v}^* = \overline{F_x} + \left(\frac{K_b f_o^2}{N^2}\overline{u}_z\right)_z, \tag{12}$$

which is equivalent to Eq. (24) in Gent et al. (1995). It shows that in this limit the eddy potential vorticity flux is equivalent to a vertical diffusion of zonal momentum with a coefficient $K_b f_o^2/N^2$. This has been discussed previously; see, for example, Rhines and Holland (1979), Rhines and Young (1982), Greatbatch and Lamb (1990), and Marshall et al. (1993).

In Gent and McWilliams (1990) the momentum equations are not transformed. They remain the Eulerian mean equations with the Reynolds stresses represented by Fickian diffusion terms. Buoyancy and tracer are advected with an ''effective transport'' velocity [a term coined from Plumb and Mahlman (1987)] that is explicitly calculated from the large-scale fields. The GM parameterization scheme has been the subject of much recent discussion (see, e.g., Tandon and Garret 1996; Treguier et al. 1997; Visbeck et al. 1996) and modified approaches have been offered for prescribing the ''bolus'' velocity (e.g., McDougall and McIntosh 1996; Dukowicz and Greatbatch 1997). It is well documented that GM leads to marked improvements in the ability of height-coordinate models to capture and maintain water mass distributions: see, for example, Danabasoglu et al. (1995), Böning et al. (1995), Danabasoglu and McWilliams (1995), Robitaille and Weaver (1995), England (1995), and Hirst and McDougall (1998). However, there still remains the need for the representation of vorticity and momentum transport by geostrophic eddies. Gent and McWilliams (1996) address this issue by considering, as here, the transformed Eulerian mean equations. However, in their Eqs. (8)–(9) the residual mean circulation is not a prognostic variable as in our Eq. (9) and so has to be explicitly calculated using a closure assumption. Moreover, instead of parameterizing the eddy PV flux, they parameterize the individual components of the Eliassen–Palm momentum flux, Eq. (7), in terms of downgradient momentum diffusion together with a Coriolis term. Therefore, any unmixing of momentum—upgradient transfer—will not be captured.

3. Closing for the eddy PV flux

Flux gradient relationship for PV transfer

In the framework set out in section 2, it is not necessary to separately parameterize the transfer of momentum and buoyancy by the baroclinic eddies. This avoids the problem of how to represent the transfer of momentum by the eddy disturbances. Now only the eddy transfer of potential vorticity has to be parameterized. We assume here, and following many investigators (e.g., Green 1970; Wiin-Nielsen and Sela 1971; Rhines 1977; Marshall 1981; Rhines and Young 1982; Pavan and Held 1996; Killworth 1997; Marshall et al. 1999), that the eddy transfer of potential vorticity is directed down its mean gradient.[3] Consequently the flux is represented as

$$\overline{v'q'} = -K\overline{q}_y, \tag{13}$$

where the K are eddy transfer coefficients of potential vorticity, which can vary spatially and temporally (Green 1970). Details of the computation of the mean potential vorticity $\overline{q}$ used in the model are given in the appendix.

As stressed in Marshall (1981), any parametric representation of the eddy flux of potential vorticity must be applied with care: Eq. (8) must be satisfied. That is, the total zonal momentum can be changed only by external forces and friction, and not by internally generated baroclinic eddies. This provides an integral constraint on the eddy PV flux term and hence, combining Eq. (8) and Eq. (13), on the K

$$\int_{-H}^{0}\int_{0}^{L_y} K\overline{q}_y\, dy\, dz = 0. \tag{14}$$

The transfer coefficients must be chosen in order to

[3] This assumption remains highly controversial. Circumstances can arise in which it is not true. It may be useful to regard Eq. (13) as a definition, and then the debate revolves around the transfer coefficient K—is it positive, and how does it depend on large-scale properties of the flow? But we will show, by diagnosis of the eddy-resolved channel flow described in section 4, that K is indeed positive in that simple case and has a form that is plausible and understandable.

satisfy Eq. (14). There is one constraint and, so, one free parameter. We choose to specify the K as follows:

$$K(y, z, t) = \kappa_{\text{ref}} Y(y) T(t) \left(1 + \gamma \frac{z}{H}\right). \qquad (15)$$

Here κ_{ref} is a reference value that depends on the nature of the flow (e.g., as in Visbeck et al. 1996), $Y(y)$ prescribes the meridional structure, and $T(t)$ the temporal form. The vertical structure is assumed to be linear with a scale height of H/γ, where H is the total depth of the fluid and γ is the free parameter, which will be chosen so that Eq. (14) is satisfied.

In the experiments to follow the focus will be upon incorporating the often-neglected eddy relative vorticity fluxes, so more completely representing the transfer characteristics of the eddies. However, it will prove useful to consider the limit in which eddy relative vorticity fluxes are neglected—as discussed in section 2b. In this case the PV is evaluated using the stretching term only and the absolute vorticity is set to zero [see Eq. (A2) in the appendix]. The GM parameterization in the zonal average can then be interpreted as a limit case of PV transfer. The vanishing of the stretching term when vertically integrated is guaranteed because of the use of Bretherton PV sheets at the top and bottom. As a result, in this limit there is no need to vary K spatially to satisfy zonal momentum constraints, and it is therefore set to a constant value. Before going on, however, we emphasize that we do not employ a closure for the buoyancy flux [Eq. (10)] in this study, but always work in terms of eddy PV fluxes (13)—the limit of vanishing eddy relative vorticity fluxes is obtained by setting absolute vorticity gradients to zero when evaluating PV gradients in the parameterized model.

With knowledge of the transfer coefficients K, Eq. (13) closes for the eddy potential vorticity flux, and thus the divergence of the Eliassen–Palm flux. We now go on to describe how the above parameterization scheme represents the eddy–mean flow interaction in an eddying, β-plane channel.

4. Parameterization of eddies in a stress-driven channel

To illustrate the ideas outlined in section 2 and to test the approach to parameterization presented in section 3, we present calculations with a three-dimensional numerical model that resolves the baroclinic eddy field. We compute the eddy statistics of interest, average zonally, and consider them in light of the theoretical ideas reviewed in sections 2 and 3. We then compare the resolved model with a zonally averaged one that implements TEM with eddy-PV flux forcing. The numerical model used is that of Marshall et al. (1997a,b).

TABLE 1. Parameters for the stress-driven channel expts.

Parameter	Units	Eddy-resolving model	Parameterized model
f_0	s^{-1}	1×10^{-4}	1×10^{-4}
Wind stress, τ	Pa	0.2	0.2
Bottom drag	s^{-1}	1×10^{-5}	1×10^{-5}
x domain (L_x)	km	1500	—
y domain (L_y)	km	500	500
Depth	m	4500	4500
Horizontal grid size	km	20	20
Vertical grid size	m	50–400	400
Vertical levels		21	12
Initial stratification (N/f_0)		21	21
Rossby radius (NH/f)	km	95	95
Horizontal diffusivity	$m^2\ s^{-1}$	0	0
Biharmonic diffusivity	$m^4\ s^{-1}$	0	0
Vertical diffusivity	$m^2\ s^{-1}$	0	0
Horizontal viscosity	$m^2\ s^{-1}$	0	0
Biharmonic viscosity	$m^4\ s^{-1}$	1×10^{11}	1×10^{11}
Vertical viscosity	$m^2\ s^{-1}$	0	0
κ_{ref}	$m^2\ s^{-1}$	—	1050
$T(t)$		—	Linear ramp: 30 days
$Y(y)$		—	0, $y = 0$, L_y
		—	1, $0 < y < L_y$

a. Flow in a stress-driven β-plane channel

We simulate the wind-driven flow of an ocean in a periodic channel on a β plane of width 500 km, length 1500 km, and depth 4500 m. The calculation can be regarded as a primitive equation counterpart of the kind studied by McWilliams et al. (1978) quasigeostrophically. It can be considered to be an analogue of a segment of the Antarctic Circumpolar Current, although here our jet is in the northern hemisphere! A wind stress is applied to the upper level of the model of sinusoidal form:

$$\tau = \tau_o \sin\left(\frac{\pi y}{L_y}\right).$$

It has a maximum value of 0.2 Pa at the center of the channel and is zero at the side walls. The initial stratification is constant. The vertical grid spacing is 50 m in the upper layer and increases to 400 m in lower layers. Friction is present through a bottom drag in the lower layer. Biharmonic viscosity and diffusion suppress numerical noise on the grid scale. There is no thermodynamic forcing ($G = 0$) and no Fickian diffusion terms. Static instability is released by convective adjustment. The numerical experiments carried out in this section are summarized in Table 1. The equation of state is a linear function of temperature, so, henceforth, our discussion will be in terms of temperature and temperature flux alone.

Before examining the statistically steady-state solution we consider the spinup of the model from rest. The

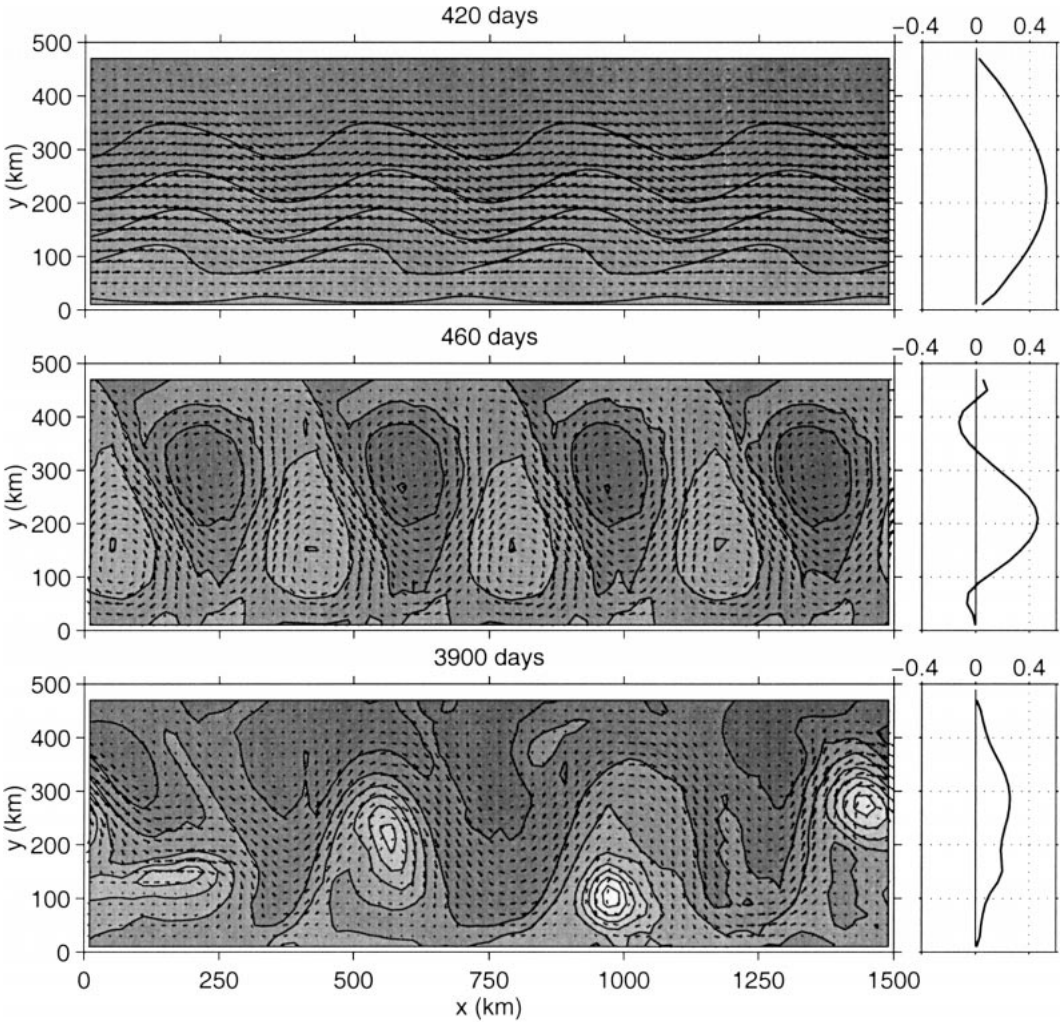

FIG. 1. Surface velocities from the eddy-resolving channel model after 420, 460, and 3900 days. The temperature is contoured and shaded with lighter shading denoting warmer water. The panels on the right display the corresponding zonal mean zonal surface velocity in meters per second.

time development of the surface temperature and velocity fields is shown in Fig. 1. The wind stress drives a southward Ekman flow in the upper layer that returns northward in an Ekman layer at the bottom. This results in downward Ekman pumping in the southern half of the channel and Ekman suction to the north. The resulting meridional overturning leads to a deepening of isotherms in the south and a shoaling to the north. In this way a lateral temperature gradient develops across the channel that supports a surface-intensified jet in thermal wind balance. After a year or so the jet develops growing meanders due to baroclinic instability, as shown in Fig. 1a. These eddies continue to grow, releasing available potential energy as they reach finite amplitude (Fig. 1b) until wave breaking occurs and coinciding with a conspicuous decrease in the zonal velocity of the jet. Following the initial instability the eddy field exhibits more irregularity with a broader spectrum of sizes. Finally, after six years or so (see Fig. 1c) a statistically steady state is reached in which the input of potential energy by the wind is equilibrated by its release through baroclinic instability.

1) EQUILIBRATED STATE

The model was integrated for 20 years and the statistically steady state was reached after approximately 6 years. The time average was obtained by averaging the last 10 years of integration. The zonal mean zonal velocity in the equilibrated state is characterized by a surface-intensified jet (Fig. 2a) in thermal wind balance with the temperature field (Fig. 2b). Maximum surface velocities are 0.24 m s^{-1} in midchannel, reducing to zero at the side walls. The Eulerian mean meridional streamfunction is plotted in Fig. 3a and is that of the stress-driven Ekman flow. It consists of southward transport at the surface with sinking in the south and northward return flow at depth. This Eulerian mean flow

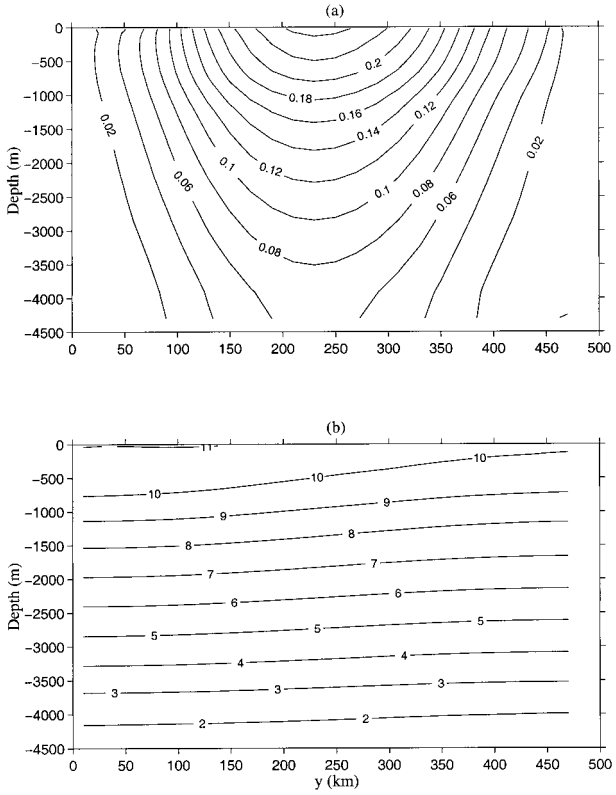

FIG. 2. Zonal-average fields from the β-plane eddy resolving channel model. The time-averaged meridional cross sections of (a) zonal mean zonal velocity (m s^{-1}) and (b) zonal mean temperature. The time average was taken from 10 to 20 years.

deepens the isotherms in the south and shoals them to the north, acting to increase the meridional temperature gradient. This stress-driven overturning rate has a maximum in midchannel of 4.00 Sv (Sv $\equiv 10^6$ m^3 s^{-1}). However, in the transformed Eulerian mean framework, Eq. (4d) states that

$$\overline{v}^*\overline{T}_y + \overline{w}^*\overline{T}_z = 0 \tag{16}$$

in the equilibrated state. If we write the residual mean circulation in terms of a streamfunction,

$$\chi^* = \chi_{\text{Eul}} + \chi_{\text{flux}},$$

where χ_{Eul} is the Eulerian mean streamfunction and $\chi_{\text{flux}} = (\overline{v'b'}/N^2)$ is the streamfunction associated with buoyancy flux terms, then Eq. (16) can now be restated as

$$J(\chi^*, \overline{T}) = 0. \tag{17}$$

For our stress-driven channel, the only physical solution to Eq. (17) has the streamlines coincident with the isotherms. Since the isotherms intersect the vertical walls where $\chi^* = 0$, the result is that $\chi^* = 0$ everywhere. Thus the residual mean overturning circulation has vanished. The wind-driven Eulerian mean circulation is exactly canceled by the terms involving the buoyancy fluxes in Eq. (2a–b). The streamfunction χ_{flux} is diagnosed directly from the model using the eddy buoyancy fluxes and the horizontal mean N^2 profile, and is plotted in Fig. 3b. It is almost everywhere equal and opposite to χ_{Eul} (Fig. 3a). At any latitude χ_{flux} is constant with height except for the upper and lower 500 m in the channel center. This overturning rate has a maximum in midchannel of 3.98 Sv. For the turbulent, nonlinear, primitive equation eddy resolving flow under consideration here there exists a very small nonzero residual mean circulation (over the time interval of the time averaging), the running average of which asymptotes to zero. Thus the TEM framework provides a clear understanding of the equilibrated zonal mean fields of the stress-driven channel.

2) EDDY STATISTICS AND TRANSFER CHARACTERISTICS

Vorticity and potential vorticity fluxes. In the steady state the depth integral of the zonal momentum equation, (4a), is

$$\int_{-H}^{0} \overline{v'q'}\, dz = \int_{-H}^{0} -\frac{\partial}{\partial y}\overline{u'v'}\, dz = -\int_{-H}^{0} \overline{F}^x\, dz, \tag{18}$$

and integrating over the volume of the channel we have

$$\int_V \overline{F}^x\, dV = 0.$$

Note that at any latitude, however, $\int_{-H}^{0} \overline{F}^x\, dz \neq 0$; the bottom stress does not exactly balance the surface stress. Their difference is equal to the vertically integrated potential vorticity flux, which itself is exactly equal to the vertically integrated relative vorticity flux (see Fig. 4). For reasons which are well known,[4] eddies pump eastward momentum in to the jet, taking it from the flanks. The net effect of the eddy vorticity transfer, then, is to sharpen the jet with momentum being transferred up its large-scale gradient.

Figure 6a plots the meridional profile of $\overline{v'q'}$ deduced according to Eq. (5) and shows that eddies exert a positive (eastward) body force in the lower sheet and a negative body force in the upper PV sheet. This can be

[4] The form of the eddy momentum flux can be understood in terms of the horizontal anisotropy of the eddies. The eddy velocities (u', v') have a zero zonal mean, but their correlation $\overline{u'v'}$ will be nonzero if the eddies are not circular. Deformation of eddies, by mean flow and Rossby wave propagation, leads to them becoming ''banana shaped'' as shown in Fig. 5. To the south of the jet axis the troughs slope in a southwest–northeast sense to give a northward eddy flux of eastward eddy zonal velocity in the zonal mean. North of the jet axis, troughs exhibit a southeast–northwest tilt resulting in a southward eddy flux of eastward eddy zonal velocity. Thus the effect of the eddies is to transfer eastward momentum into the center of the eastward jet resulting in a zonal-mean eastward body force that sharpens and intensifies the mean zonal flow in the center and decelerates it on the flanks.

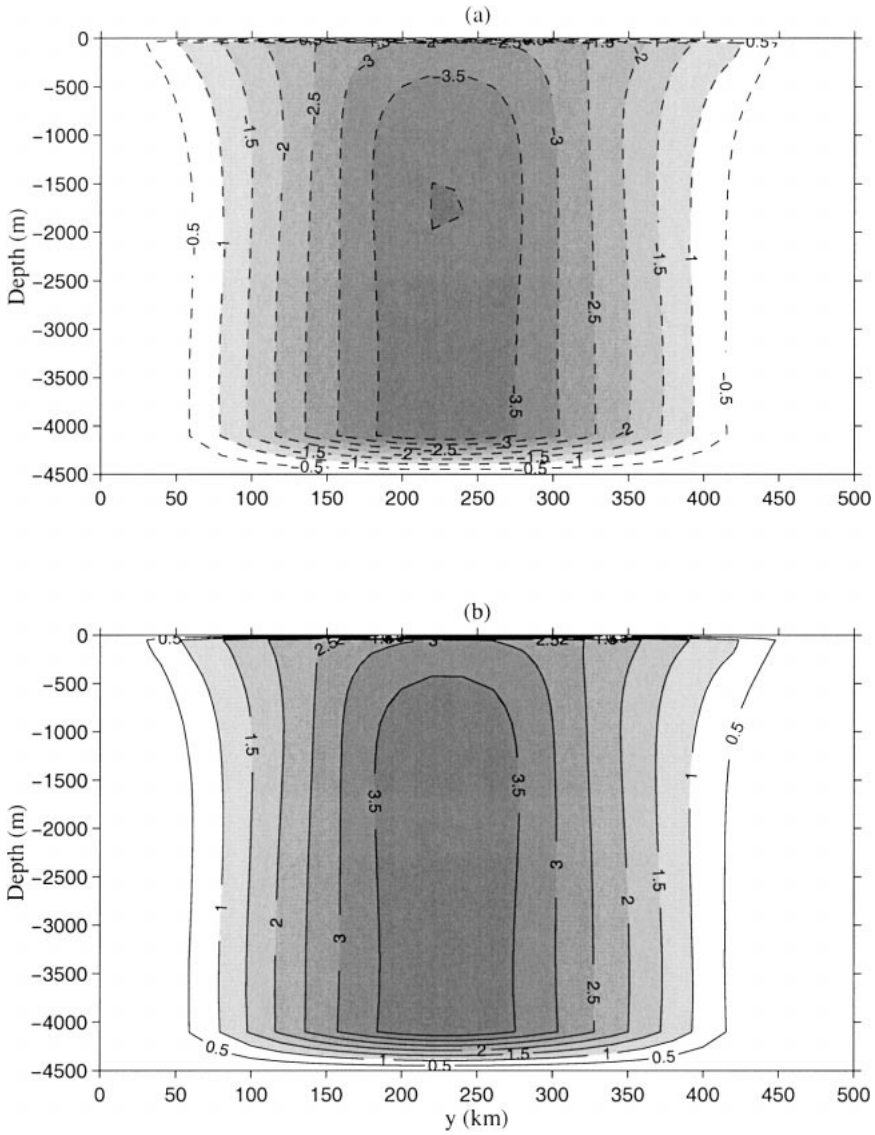

FIG. 3. The wind-driven Eulerian mean streamfunction in the eddy-resolving model, χ_{Eul}, in (a) is almost exactly canceled by χ_{flux} in (b). Units are Sverdrups (10^6 m^3 s^{-1}). The result is the near vanishing of the residual mean overturning circulation.

understood when we consider the zonal momentum balance, written thus:

$$0 = \overline{v'q'}^{xt} + \frac{1}{\rho_o}\frac{\partial \overline{\tau}^{xt}}{\partial z}, \qquad 0 = \overline{v'q'}^{xt},$$

$$0 = \overline{v'q'}^{xt} - \epsilon \overline{u}^{xt},$$

for the upper boundary, interior, and the lower boundary of the channel, respectively. Thus at the upper boundary the imposed wind stress is balanced by a southward eddy flux of potential vorticity. At the lower boundary the bottom stress is balanced by a northward eddy flux of potential vorticity. In the interior the meridional eddy flux of potential vorticity is very small and the Eliassen–Palm flux is nondivergent.

The zonal-mean eddy flux of temperature (see Fig. 6b) is almost constant with height in midchannel but varies as the surface is approached. However $\overline{v'T'}/N^2$ is almost constant with depth since N^2 is weaker in the upper km—this was exploited by Johnson and Bryden (1989) and Marshall et al. (1993) in their simplified models of the Antarctic Circumpolar Current. The temperature flux characteristics are broadly in accord with the Eady model of baroclinic instability.

Eddy transfer coefficients. We now inspect the sense of the meridional eddy flux of potential vorticity with respect to the mean PV gradients to assess whether the eddy closure hypothesis, Eq. (13), is appropriate. The meridional profile of the transfer coefficients for the upper and lower PV sheets are shown in Fig. 7. All

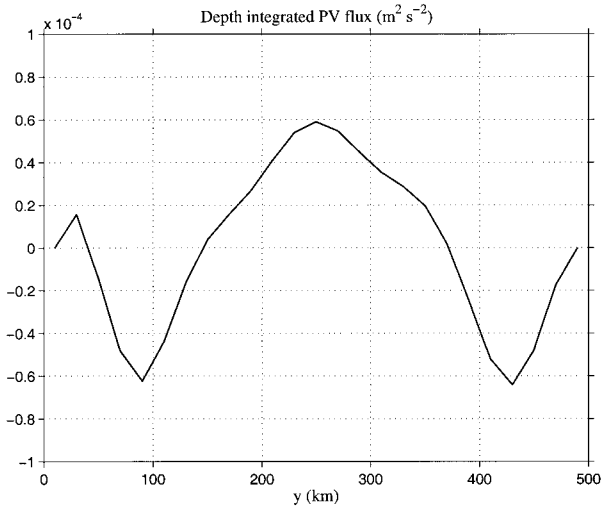

FIG. 4. The depth integrated PV flux in the eddy resolving model. At any latitude the difference between the bottom drag and surface stress is balanced by an eddy flux of PV. A positive (eastward) body force is exerted on the zonal flow in the center of the channel and a negative (westward) body force is exerted on the flanks of the jet.

values of K are positive except near the southern boundary where the sign of the mean potential vorticity gradient changes sign but $\overline{v'q'}$ does not. In the upper sheet K ranges from $\sim$200 m^2 s^{-1} in the center of the jet, where the mean PV gradients are a maximum, to $\sim$900 m^2 s^{-1} at the northern flank where the mean gradients are weaker. In the lower sheet the values of K are higher than in the upper sheet, reaching a maximum value of $\sim$6900 m^2 s^{-1} in the jet center. A local minimum is found on either side of the jet in regions where the mean potential vorticity gradients have slight maxima. Thus the form of the diagnosed transfer coefficients is rather complex with structure in both the horizontal and vertical. This complexity is further revealed when we plot $\overline{v'q'}$ against $\overline{q}_y$ for each sheet (Fig. 8). If the transfer were truly local and directed downgradient, then the slope of $\overline{v'q'}$ versus $\overline{q}_y$ would be $-K$. Figure 8 shows that the line for the upper sheet is not straight but rather doubles back to form a partly open curve suggesting that for any particular value of the gradient there are two values of eddy PV flux. This is because different values of $\overline{q}_y$ occur on either side of the jet center and have different eddy fluxes associated with them.

b. The parameterized model

The equivalent wind-driven experiment was performed in the parameterized model (see Table 1). The governing equations are given by Eqs. (9a–e), where we represent the meridional eddy flux of perturbation QG potential vorticity by a downgradient transfer of mean QG potential vorticity with the coefficient K in the form expressed by Eq. (13).

The magnitude of κ_{ref} was chosen so that the peak of the depth-integrated transport in the zonally-averaged model matched that of the eddy-resolved calculation and $Y(y) = 1$ (Table 1). As in the eddy-resolving model, the wind stress drives a southward Ekman flow in the upper level of the model, which results in downward displacement of isotherms in the southern half of the channel. The meridional flow returns within the Ekman layer at the bottom level, inducing upward isothermal displacement to the north. This gives rise to a linearly increasing lateral temperature gradient across the channel that, through thermal wind, supports a surface-intensified jet. The contribution to the quasigeostrophic PV from the

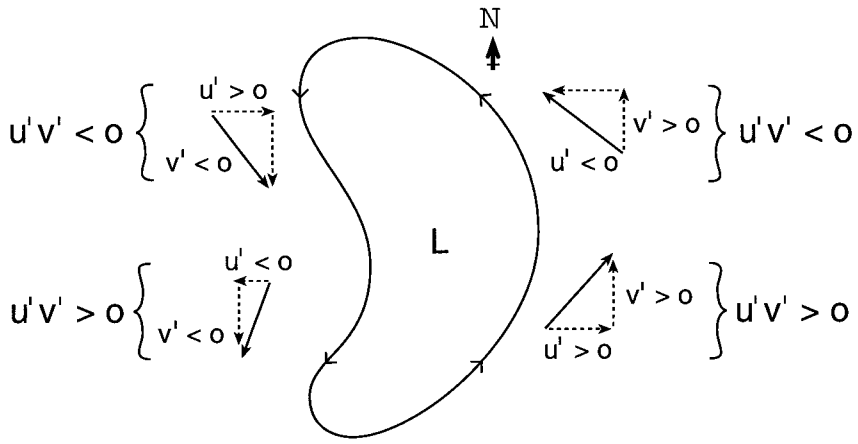

FIG. 5. Eddy momentum fluxes associated with a ''banana-shaped'' eddy. The eddy velocities (u', v') have a zero zonal mean, but their product can be nonzero if the eddy, as here, is anisotropic. To the south of the jet axis the trough slopes in a southwest–northeast sense inducing a northward eddy flux of eastward eddy zonal velocity $\overline{u'v'} > 0$. North of the jet axis, the troughs tilt southeast–northwest and $\overline{u'v'} < 0$. Thus the effect of the eddies is to transfer eastward momentum into the center of the eastward jet from the flanks. This effect is well known in the atmospheric literature (see, e.g., Starr 1968).

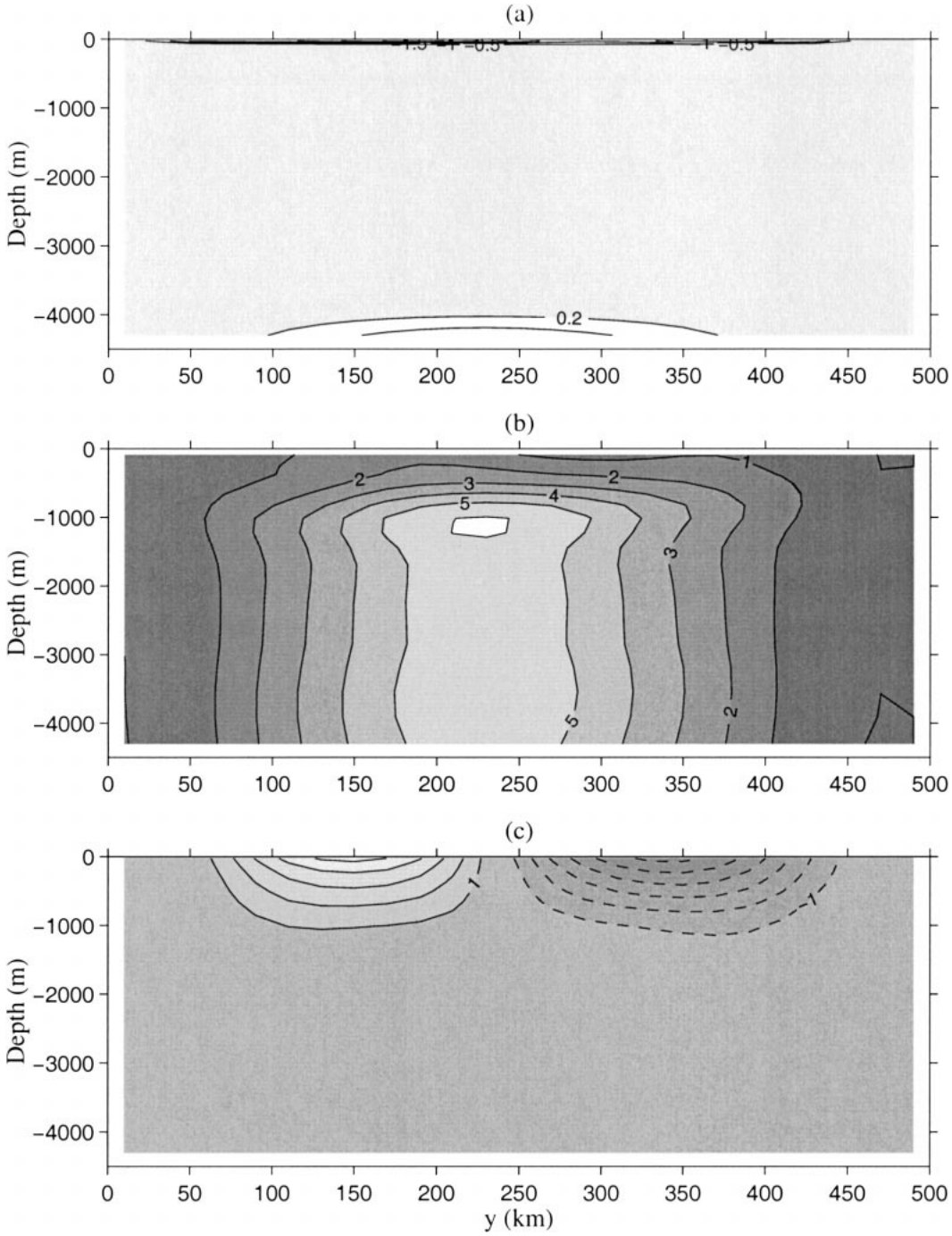

FIG. 6. Meridional cross sections of (a) the eddy-PV flux ($\overline{v'q'}^{xt}$) dominated by the boundary sheets with divergence at depth and surface convergence; (b) the eddy flux of temperature, $\overline{v'T'}^{xt}$, ci = 1×10^{-3} m s^{-1} K; (c) the eddy flux of momentum, $\overline{\mathbf{u}'v'}^{xt}$; ci = 1×10^{-3} m^2 s^{-2}.

relative vorticity and stretching terms increases as the flow field evolves. At each time step the eddy PV transfer coefficient K is calculated from the evolving fields using the momentum constraint, Eq. (14). If the necessary conditions for instability are not satisfied, [i.e., if Eq. (14) can only be satisfied if the K become negative somewhere] then K is set to zero.

As the isotherms tilt, the temperature perturbations at the lower boundary give rise to a contribution to the PV that acts to offset β, eventually leading to a reversal

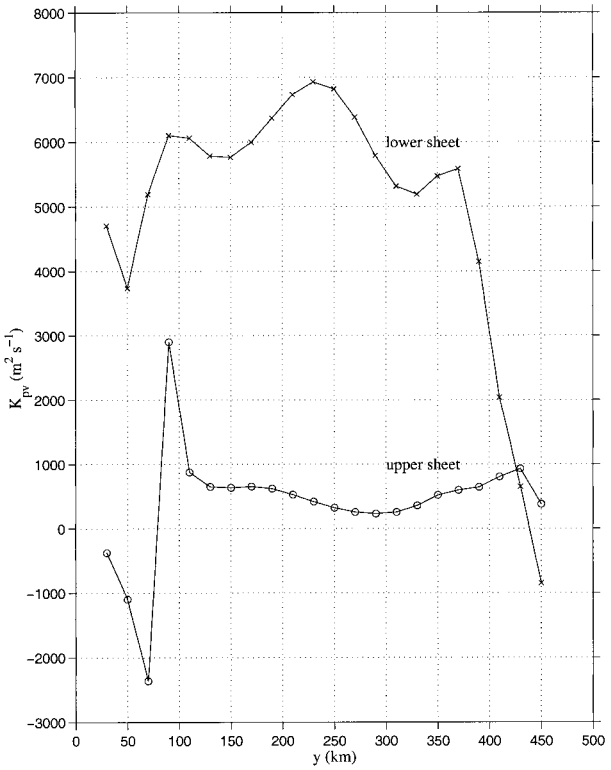

FIG. 7. The diagnosed transfer coefficients for quasigeostrophic potential vorticity in the upper PV sheet (circles) and the lower PV sheet (crosses) in the statistically steady state of the eddy resolved model.

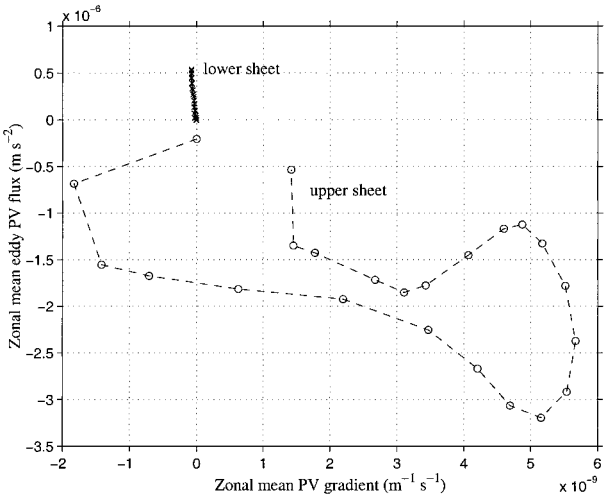

FIG. 8. Plot of $\overline{(v'q')}$ vs $\overline{q}_y$ for the PV sheets in the eddy-resolved model.

in the PV gradients. This allows the momentum constraint, Eq. (14), to be met with $K(y, z, t) > 0$ everywhere and the necessary conditions for instability to be satisfied. When the K are initially nonzero, they are increased linearly over a month to crudely simulate the growth of baroclinic instability. The evolution of the global mean K is displayed in Fig. 9a and shows that after 5 years the model is in a steady state.

The mean zonal velocity (Fig. 10a) consists of a surface-intensified jet in the channel center with weak return (westward flow) at depth on the flanks. The zonal velocity is in thermal wind balance with the temperature field shown in Fig. 10b. It compares favorably with the mean flow of the resolved calculation (see Figs. 2a,b).

The steady-state zonal momentum balance throughout the fluid is

$$0 = \overline{F}_x + \overline{v'q'}^x. \tag{19}$$

The balances in (19) are shown in Fig. 11. At the upper boundary (Fig. 11a) the wind stress is balanced by the term representing the eddy flux of QG potential vorticity, giving a sheet with a southward eddy flux of potential vorticity. At the bottom (Fig. 11c) the stress is balanced by the parameterized terms representing a northward eddy flux of potential vorticity. In the interior (Fig. 11b), there is no applied force; thus in the steady state the eddy PV flux is zero. Because of the flux gradient relationship assumed for the eddy-PV flux [Eq. (13)], this implies that the interior QG potential vorticity gradients are zero.

The reference transfer coefficient in the upper layer

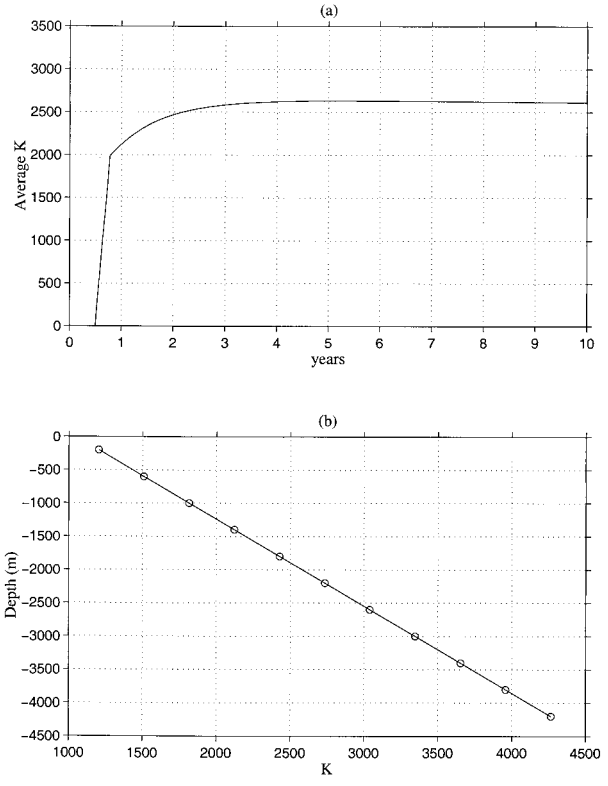

FIG. 9. (a) The time series of the global average K (m^2 s^{-1}) in the parameterized model; (b) the steady-state K profile with $\kappa_{ref} = 1050$ m^s s^{-1}.

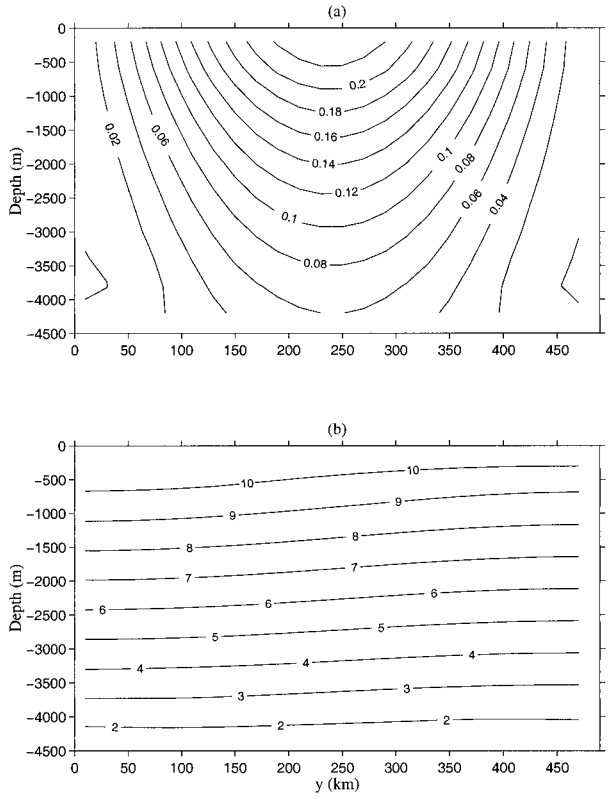

FIG. 10. Steady-state meridional cross sections from the parameterized model: (a) zonal mean zonal velocity (m s^{-1}) and (b) zonal mean temperature.

was specified to be 1050 m^2 s^{-1}. In the steady state the value of the free parameter γ in (15) was -3.21, giving

$$K = 1050\left(1 - 3.21\frac{z}{H}\right) \quad m^2\ s^{-1} \tag{20}$$

with K increasing as we move down in the column. Figure 9b shows the K profile. The transfer coefficient becomes large in the lower PV sheet to compensate for the small negative potential vorticity gradient there, just as for the K diagnosed from the resolved model. As shown in Fig. 11, $\nabla \cdot \mathbf{E}$ in the steady state consists of boundary sheets with divergence at the lower horizontal boundary and convergence at the surface. The meridional profile is shown in Fig. 12a. This is consistent with the EP signature for the eddy resolving calculation.

The depth-integrated parameterized eddy PV flux is plotted in Fig. 12b and shows that the effect of the eddies is to exert a positive (eastward) body force on the zonal momentum in the center of the jet and a negative (westward) body force on the flanks. Thus momentum is transferred upgradient into the jet center resulting in the depth-integrated zonal flow shown in Fig. 13. This agrees with diagnosed eddy forcing of the zonal mean flow from the eddy-resolving flow and demonstrates that the zonal-average model can capture this rather subtle aspect of eddy–mean flow interaction.

One shortcoming of the zonal-average model is that it fails to take into account some of the nonlocal effects. The resolved fields exhibit a change in sign of the surface quasigeostrophic potential vorticity close to the southern vertical wall, which is absent from the parameterized model. A second difference is that the magnitude of the parameterized depth-integrated eddy PV flux is 25% less than that diagnosed from the eddy-resolving calculation (Figs. 4 and 12b). The size of the potential vorticity flux in the upper sheet in each model is very similar [it has to be since it must balance the surface stress in both resolved and parameterized models; see Eq. (19)], but the magnitude of the potential vorticity flux at the bottom is underestimated in the parameterized model. Since this flux acts to balance the bottom drag, the velocities at depth in midchannel are smaller for the parameterized model, as can be seen by comparing Figs. 2a and 10a, even though the depth-integrated zonal mean flow are very similar. Consequently the depth integral of the potential vorticity flux is smaller in the parameterized model compared to the eddy-resolved model.

Despite these differences, the parameterized model captures the characteristic signatures of eddy buoyancy and momentum transfer, and the zonal-mean fields and overturning circulation of the eddy-resolved calculation.

5. Spindown of a baroclinic zone on a β plane

We now consider, following Gent et al. (1995) and Visbeck et al. (1996), the spindown of a baroclinic zone in the absence of external buoyancy forces. Again, we compare calculations from the three-dimensional numerical model that resolves the baroclinic eddy field to the zonal average model in which we parameterize the eddy–PV transfer.

The sloping baroclinic zone is characterized by the meridional temperature profile displayed in Fig. 14. The initial stratification is of constant value in the vertical. The slope is uniform in the y direction except at the walls where the isotherms flatten. The isotherms intersect the surface of the channel and ''ground out'' at the lower boundary. The model has 20 active levels in a periodic channel of length 750 km, width 250 km, and depth 4500 m and was integrated for 10 years (see Table 2).

The time evolution of the eddy-resolved flow is summarized in Fig. 15, which shows surface temperature and velocity fields at time 165, 180, 240, and 3600 days. Initially, the alongchannel velocity has maxima of approximately 0.9 m s^{-1}. The front becomes baroclinically unstable after approximately 165 days. By day 180 finite amplitude eddies fill the channel. These are organized to give a cross-zone ageostrophic flow that transfers fluid from one side of the channel to the other. In the northern half of the channel downwelling draws cold

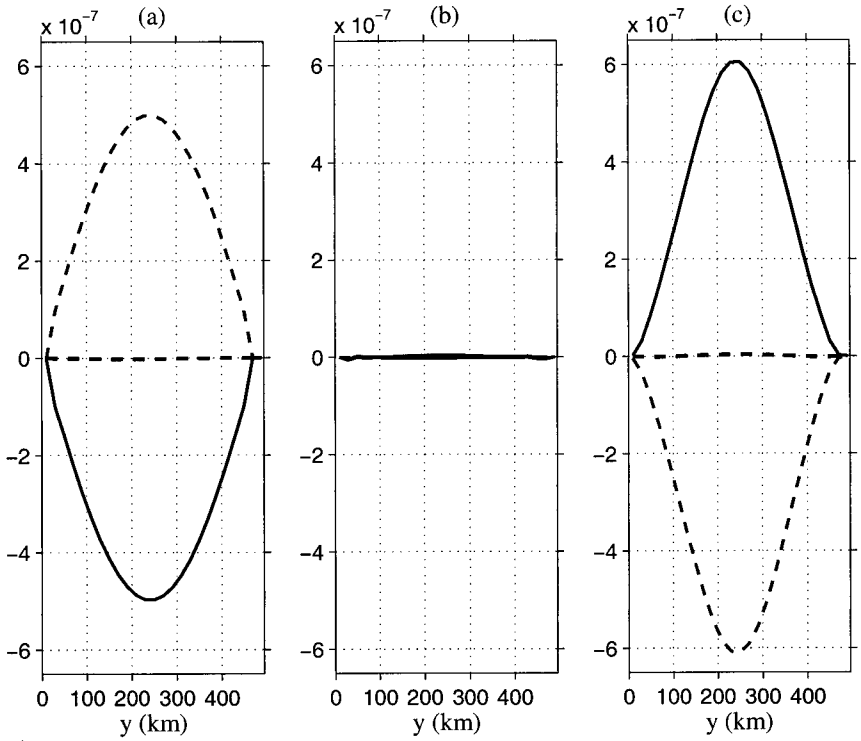

FIG. 11. The stress (dashed) and $\overline{v'q'}$ (solid) terms in the steady-state momentum equation of the parameterized model for (a) the upper-PV sheet, (b) the interior, and (c) the lower-PV sheet. Equation (19) is exactly satisfied.

water down, while to the south the isotherms are raised. This results in a release of the mean potential energy stored in the sloping density surfaces. The baroclinic eddies, drawing their kinetic energy from potential energy release, spin down the zonal jet. Eventually the available potential energy stored in the sloping isotherms can no longer be released and eddy generation ceases. With the instability shut off, a baroclinically stable zonal end-state remains: see the surface flow at 3600 days (Fig. 15c). The final state is shown in Fig. 16 and is obtained from time averaging the last 3 years of model time. Averaging the three-dimensional fields along the front in the equilibrated state yields a surface-intensified jet with alongfront peak velocity of 0.14 m s^{-1} in the center of the channel (see Figs. 16b,c). The jet is in thermal wind balance with the temperature field shown in Fig. 16b.

The parameterized model

The 2D model was employed for the same problem and initialized with the same meridional temperature profile. Unlike in section 4, here the eddies and their parameterized fluxes are only present in the transient stage of flow. However, the final state depends on the eddy transfers during the transient phase.

The PV gradients in the interior are essentially set by the planetary vorticity gradient, β, with relative vorticity contributing as the side walls are approached. To the south at all depths the fluid is warmer than if the isotherms were horizontal, while to the north the temperatures are cooler. The attendant temperature perturbations along the upper and lower boundaries are associated with PV gradient sheets that oppose one another and satisfy the necessary conditions for baroclinic instability.

The evolution of the zonally averaged flow closely obeys the momentum balance:

$$\overline{u}_t - f\overline{v}^* = \overline{v'q'} - \epsilon\overline{u},$$

where $\epsilon\overline{u}$ is only operative at the bottom level of the model. In the model the primary momentum balance is between the Coriolis and eddy flux terms with the zonal momentum tendency being the residual between the two. The meridional velocity is northward in the upper sheet, enabling the Coriolis term to balance the meridional potential vorticity flux. In the lower sheet the zonal momentum tendency is the residual of the balance between the Coriolis, eddy flux, and bottom drag terms. The meridional velocity is southward here. In the interior the zonal mean flow is accelerated by the residual between Coriolis forces and eddy PV forcing. Thus a residual mean circulation is established that acts to overturn the fluid.

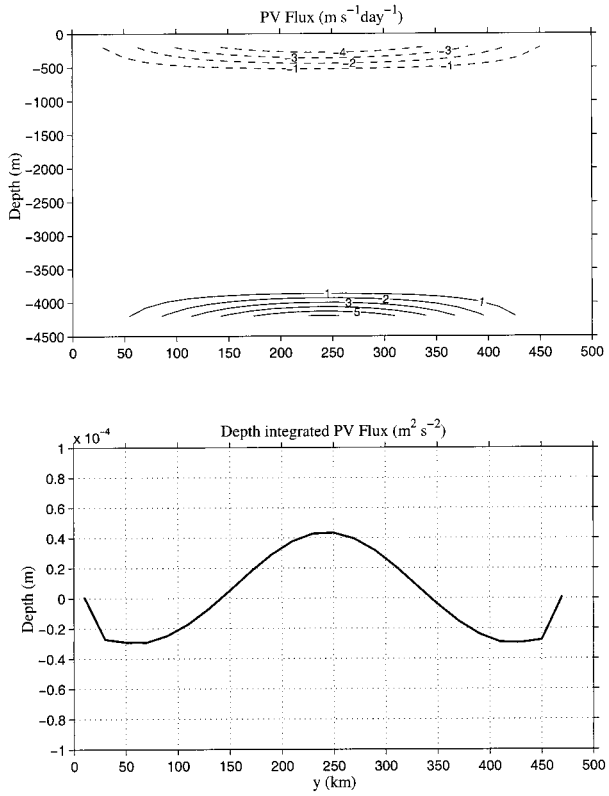

FIG. 12. (a) The PV flux ($\overline{v'q'}$) for the parameterized model; (b) the depth integrated PV flux. Its effect is to exert a positive (eastward) body force on the zonal momentum in the center of the channel, and a negative (westward) body force in the flanks of the jet, consistent with the eddy characteristics diagnosed from the eddy-resolving model.

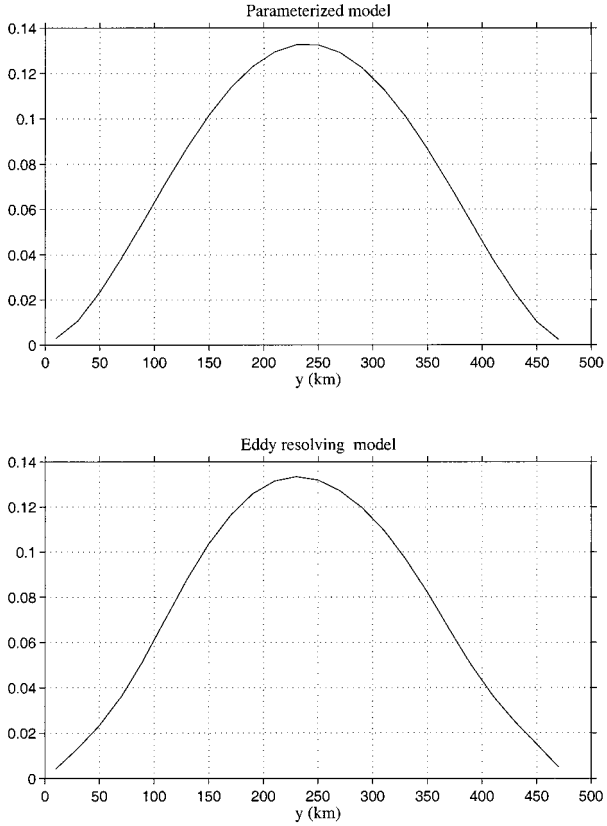

FIG. 13. The depth average of the zonal mean zonal velocity in the (a) parameterized model and (b) eddy-resolving model.

The residual mean circulation draws the warmer water in the south upward, and the colder water to the north downward, releasing available potential energy and spinning down the zone. This continues until the component of the PV gradients associated with the temperature perturbations of the sheets at the lower boundary are too weak to offset β. At this point the necessary conditions for baroclinic instability are no longer satisfied and further spindown ceases due to the stabilizing effect of the planetary vorticity gradient. The end-state is baroclinically stable zonal flow: see Fig. 17. The peak velocity at the surface is 0.142 m s^{-1}, similar to the along-zone maximum found in the eddy-resolving calculation. However, when compared to the eddy-resolving calculation, the parameterized model has stronger flows at depth, as can be seen by comparing Figs. 16 and 17.

We now consider the limiting case of zero relative vorticity fluxes, as discussed in section 2c(2). If relative vorticity fluxes are set to zero in Eq. (5), then Eq. (14) is automatically satisfied at each latitude y in the channel by the upper and lower PV sheets. A constant value of K is used, as in GM. The initial fields satisfy the necessary conditions for baroclinic instability, so the evolution of the flow proceeds as before. However, as the zone spins down, the gradients of the temperature perturbation on each boundary continue to decrease because there is no stabilizing absolute vorticity gradient. The final state of the zone is shown in Fig. 18; the parameterized model has adiabatically flattened the isotherms until the zone is horizontal with no zonal flow, the limit that would be obtained using GM.

6. Atmospheric jet stream

Tropospheric eddies in the atmosphere

The troposphere provides a very interesting test of the theoretical ideas outlined in sections 2 and 3 because baroclinic eddies are the most important component of the atmospheric general circulation outside of the tropics (Jeffreys 1926; Starr 1948; Lorenz 1967). The net radiative budget of the earth–atmosphere system, averaged over a year, results in a net surplus of incoming radiation in the Tropics and a net deficit at high latitudes. Thus for the global climate to be in equilibrium there must be transport of energy from low to high latitudes in order to balance the terrestrial radiation budget. Extratropical transport occurs through motions generated

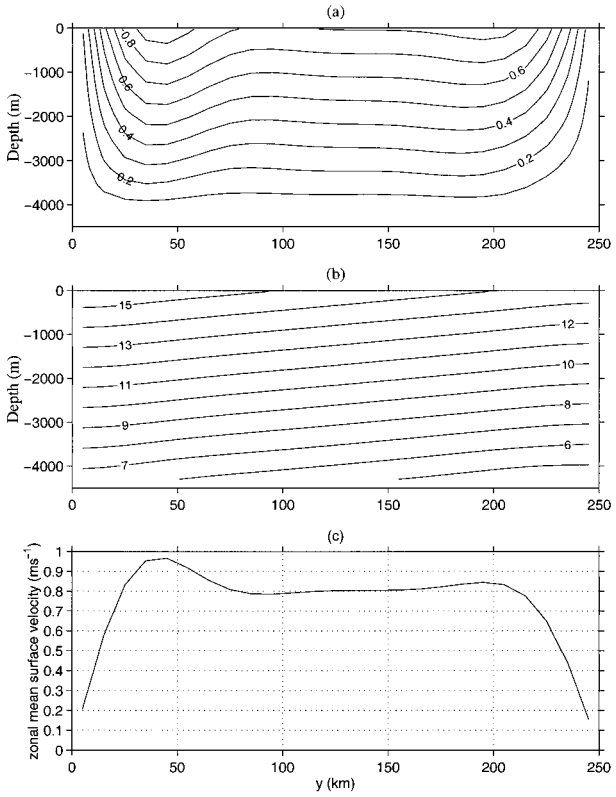

FIG. 14. The initial state of the baroclinic spindown problem: (a) zonal velocity, (b) temperature, and (c) zonal mean zonal surface velocity in the eddy-resolved model.

by the baroclinic instability of the midlatitude zonal flow. But the instability also helps maintain the zonal mean through both eddy heat and momentum fluxes.

We present three experiments here with a zonally averaged TEM atmospheric model: (i) no eddy forcing, (ii) eddy-PV forcing, and (iii) eddy-PV forcing in the absence of relative vorticity fluxes. The model solves the governing equations for an ideal gas atmosphere in hydrostatic balance. The hydrodynamical core is that of the MIT ocean model, but we employ isomorphisms to yield a p-coordinate model applicable to the flow of a compressible atmosphere (see Brugge et al. 1991). Potential temperature θ replaces b in the thermodynamic equation, Eq. (4d). Forcing is through relaxation of θ to a prescribed ''radiative equilibrium'' temperature $\overline{\theta}_{\text{eq}}(p, y)$ on a timescale $\tau(p, y)$ that are both functions of pressure and latitude (Held and Suarez 1994). Thus the potential temperature equation takes the form

$$\overline{\theta}_t + \overline{v}^*\overline{\theta}_y + \overline{w}^*\overline{\theta}_p = -\frac{1}{\tau}(\overline{\theta} - \overline{\theta}_{\text{eq}}).$$

Surface drag is represented through a quadratic drag law and there is no orography.

Five model levels are used, the lowest being at 950 mb, at the top of the surface boundary layer, and the highest at 75 mb, in the stratosphere. The parameters used in these experiments are summarized in Table 3.

TABLE 2. Parameters for the spindown of a baroclinic zone expts.

Parameter	Units	Eddy-resolving model	Parameterized model
f_0	s^{-1}	1×10^{-4}	1×10^{-4}
Bottom drag	s^{-1}	1×10^{-5}	1×10^{-5}
x domain (L_x)	km	750	—
y domain (L_y)	km	250	250
Depth	m	4500	4500
Horizontal grid size	km	10	10
Vertical grid size	m	50–400	50–400
Vertical levels		21	21
Initial stratification (N/f_0)		21	21
Rossby radius (NH/f)	km	95	95
Horizontal diffusivity	$m^2\ s^{-1}$	0	0
Biharmonic diffusivity	$m^4\ s^{-1}$	0	0
Vertical diffusivity	$m^2\ s^{-1}$	0	0
Horizontal viscosity	$m^2\ s^{-1}$	0	0
Biharmonic viscosity	$m^4\ s^{-1}$	2×10^{10}	2×10^{10}
Vertical viscosity	$m^2\ s^{-1}$	0	0
κ_{ref}	$m^2\ s^{-1}$	—	15
$T(t)$		—	Linear ramp: 100 days
$Y(y)$		—	0, $y = 0$, L_y
		—	1, $0 < y < L_y$

The initial state is a horizontally stratified atmosphere as shown in Fig. 19a, which is then relaxed to the prescribed radiative–convective equilibrium profile, $\overline{\theta}_{\text{eq}}$, on a spatially dependent timescale τ, (Figs. 19b,c). Results are presented at equilibrium, after roughly 1000 days of integration. The zonal momentum constraint is applied independently over each hemisphere to ensure that the eddy transfers in one hemisphere are independent of the PV gradients in the other hemisphere and a β-plane geometry is used.

1) NO EDDY-FORCING

The importance of the eddy forcing of the atmospheric general circulation can be most readily seen by suppressing the transfer of momentum and potential temperature by the eddies (i.e., setting $\overline{v'q'} = 0$) and inspecting the large-scale flow that occurs in their absence. The resulting flow is axisymmetric consistent with the imposed radiative forcing and the subsynoptic mixing present in the absence of the large-scale eddies.

The potential temperature, zonal velocity, and meridional circulation profiles are shown in Fig. 20. The potential temperature has relaxed to the prescribed profile resulting in a zonal velocity consisting of two westerly jets with maxima aloft at 25° latitude. Zonal velocities at 950 mb (Fig. 20d) vary between easterlies of -0.6 m s^{-1} and westerlies of 0.35 m s^{-1}. Since the eddy flux of quasigeostrophic potential vorticity is zero, the re-

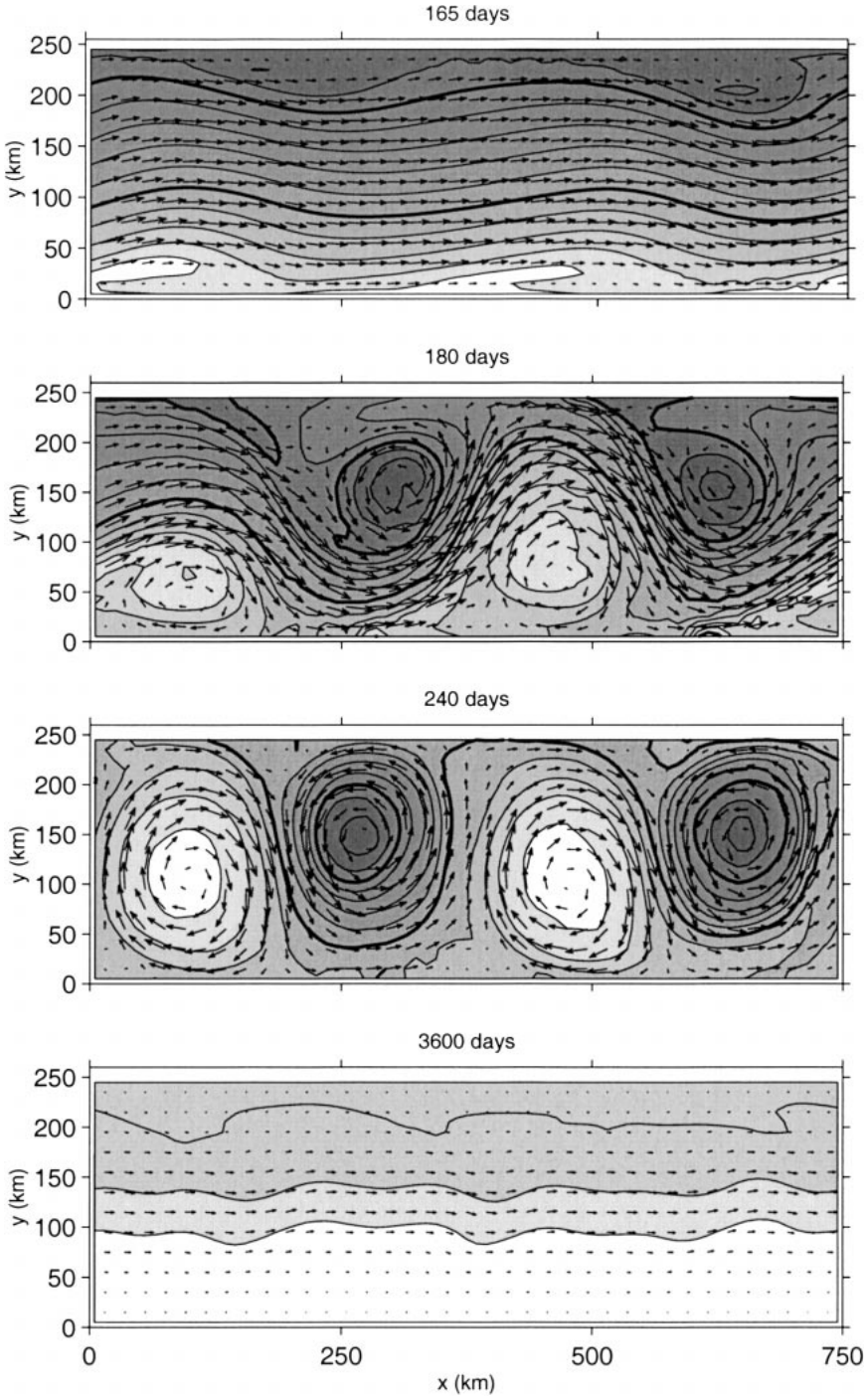

FIG. 15. Spindown of a baroclinic zone in the eddy resolved model. Surface temperature and velocities from the eddy-resolving channel model after 165, 180, 240, and 3600 days. The temperature is contoured and shaded with lighter shading denoting warmer water.

sidual mean circulation is exactly equal to the Eulerian mean circulation and this zonally averaged meridional circulation appears as Hadley cells in each hemisphere (see Fig. 20c). Low-level winds are very weak, easterly at the equator where the warm air rises and westerly at low levels where the air in the Hadley cell subsides; the net torque on the atmosphere is zero, as is required in the steady state. In the extratropics because of angular momentum constraints there is no meridional motion. The equilibrium zonal flow and potential temperature

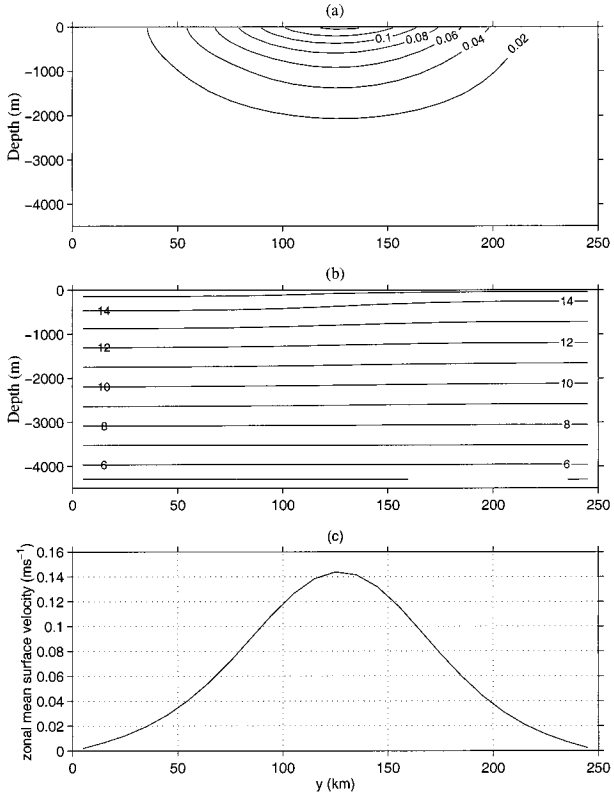

FIG. 16. Spindown of a baroclinic zone. Zonal average fields from the eddy resolving model. The time-averaged meridional cross sections of (a) zonal mean zonal velocity (m s^{-1}), (b) zonal mean temperature, and (c) zonal mean surface velocity (m s^{-1}). The time average was taken over the last three years of integration.

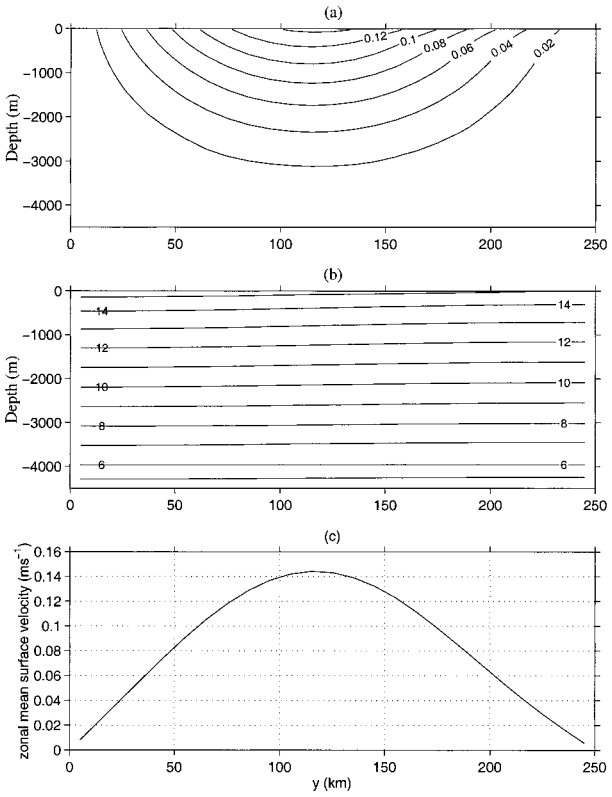

FIG. 17. Spindown of a baroclinic zone in the paramterized model. The final-state meridional cross sections of zonal average fields: (a) zonal mean zonal velocity (m s^{-1}), (b) zonal mean temperature, and (c) zonal mean surface velocity (m s^{-1}).

fields are set by the nature of the restoring terms (Held and Hou 1980).

2) EDDY FORCING

The approach of sections 2 and 3 is now employed. The reference value of the transfer coefficient is prescribed to be $\kappa_{\text{ref}} = 1 \times 10^6$ m^2 s^{-1} with the model evaluating K at each latitude and pressure in the manner described in sections 3 and 4. Again, if the potential vorticity distribution does not satisfy the necessary conditions for instability then the K are set to zero and the eddies do not force the mean flow. Once the midlatitude jets can support baroclinic instability the K become nonzero and are linearly ramped up over a 30-day period. This crudely simulates the growth of eddies whose flux will grow as they reach finite amplitude. Issues concerning the definition of the PV at the equator are circumvented by the K being zero there through the prescription of $Y(y)$; see Table 3.

In the steady state the flow in both hemispheres is characterized by westerly jets with maxima of 35 m s^{-1} at about 38° latitude near the tropopause (Fig. 21). Zonal velocities at 950 mb display equatorial easterlies of -5.1 m s^{-1}, midlatitude westerlies of 6.0 m s^{-1}, and weak polar easterlies. The residual mean streamfunction consists of a single overturning cell in each hemisphere extending farther poleward than the Hadley cells in the previous experiment. However, we emphasize that these cells are not the Hadley cells that appear in the Eulerian mean formalism; they are the cells of the transformed Eulerian mean. The potential temperature relaxation leads to diabatic heating in the Tropics where fluid parcels rise and cooling at high latitudes where they subside. Thus the residual mean circulation approximately represents the mean motion of the air parcels. It is poleward aloft with return flow at low levels. In our channel ocean experiments there were no sources or sinks of temperature, the motion was adiabatic and hence the residual mean overturning motion vanished. Here the meridional motion does not vanish due to diabatic forcing.

The eddy PV flux in the meridional plane is plotted in Fig. 22a. At the surface there is a potential vorticity sheet due to the presence of potential temperature perturbations along the boundary. There is a northward potential vorticity flux corresponding to Eliassen–Palm flux divergence. The compensating convergence occurs at most heights in the extratropical troposphere. This map of eddy PV flux agrees well both in form and

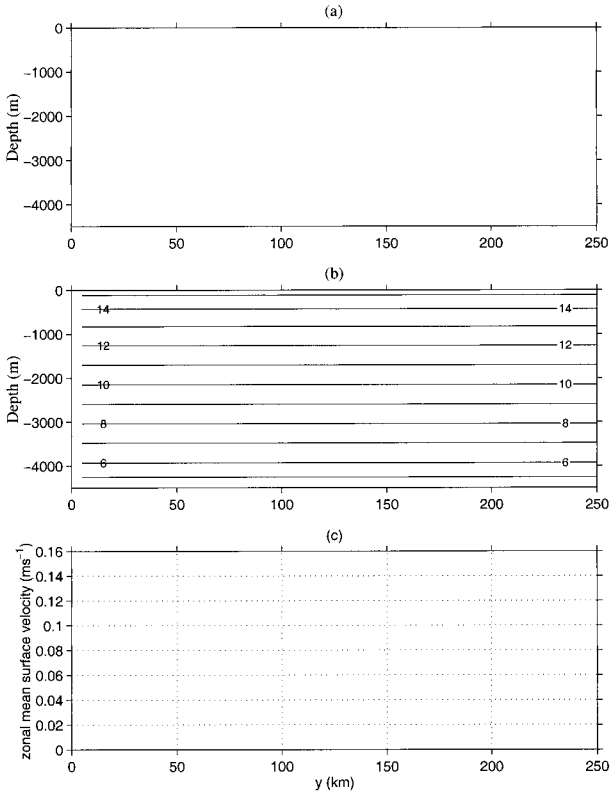

FIG. 18. Spindown of a baroclinic zone in the parametrized model. Zonal average fields from the parameterized model when relative vorticity fluxes are set to zero. The final-state meridional cross sections of (a) zonal mean zonal velocity (m s^{-1}), (b) zonal mean temperature, and (c) zonal mean surface velocity (m s^{-1}).

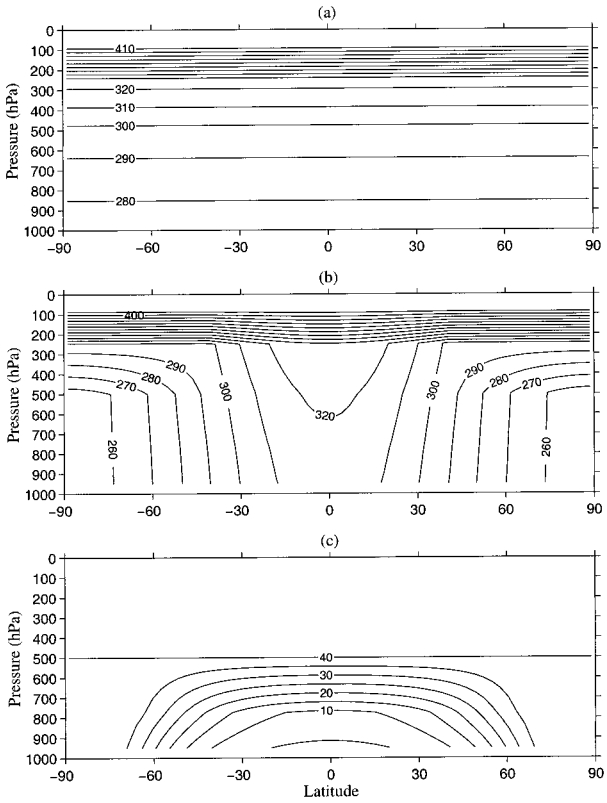

FIG. 19. Initial meridional cross sections for the troposphere experiments: (a) potential temperature, (b) $\overline{\theta}_{eq}$ the relaxation potential temperature, and (c) τ the relaxation timescale in days.

magnitude with maps diagnosed from atmospheric analyzed fields (see, e.g., Schubert et al. 1990). Integrating the zonal momentum equation over each column gives a three-way balance between the eddy-forcing term, the meridional advection of zonal flow by the residual mean ($\overline{v}^*\overline{u}_y$), and the bottom drag. The column-integrated Eliassen–Palm flux divergence (Fig. 22b) is positive in midlatitudes and negative at the equator and poles. Thus there is a column-integrated E^y that is directed from midlatitudes to the equator south of the westerlies and from midlatitudes to the pole to the north; the column-

TABLE 3. Parameters for the tropospheric eddies in the atmosphere expts.

Parameter	Units	No eddy forcing	Eddy forcing	Limiting case
Bottom drag	m^{-2}	2.1×10^{-3}	2.1×10^{-3}	2.1×10^{-3}
y domain	° lat	−90 to 90	−90 to 90	−90 to 90
Height	hPa	75 to 950	75 to 950	75 to 950
Horizontal grid size	° lat	2.8125	2.8125	2.8125
Vertical grid size	hPa	100–300	100–300	100–300
Vertical levels		5	5	5
Horizontal diffusivity	m^2 s^{-1}	0	0	0
Biharmonic diffusivity	m^4 s^{-1}	2×10^{15}	2×10^{15}	2×10^{15}
Vertical diffusivity	m^2 s^{-1}	0	0	0
Horizontal viscosity	m^2 s^{-1}	0	0	0
Biharmonic viscosity	m^4 s^{-1}	2×10^{15}	2×10^{15}	2×10^{15}
Vertical viscosity	m^2 s^{-1}	0	0	0
κ_{ref}	m^2 s^{-1}	0	1×10^6	3.4×10^5
$T(t)$		—	10 day ramp	10 day ramp
$Y(y)$		—	sin(2 × lat)	sin(2 × lat)

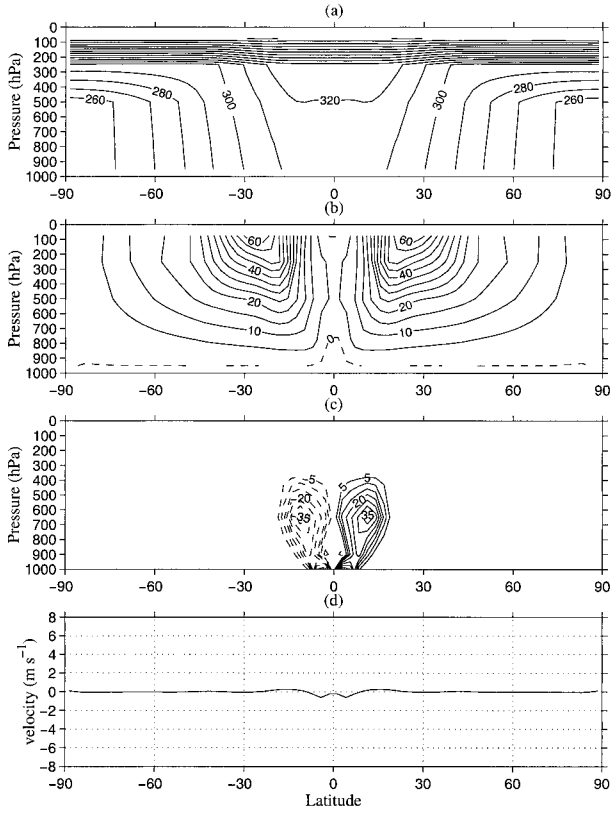

FIG. 20. The meridional cross sections after 1000 days for the experiment when $\overline{v'q'} = 0$ in the parameterized model: (a) potential temperature, (b) zonal velocity, (c) residual mean overturning streamfunction, and (d) 950-mb winds.

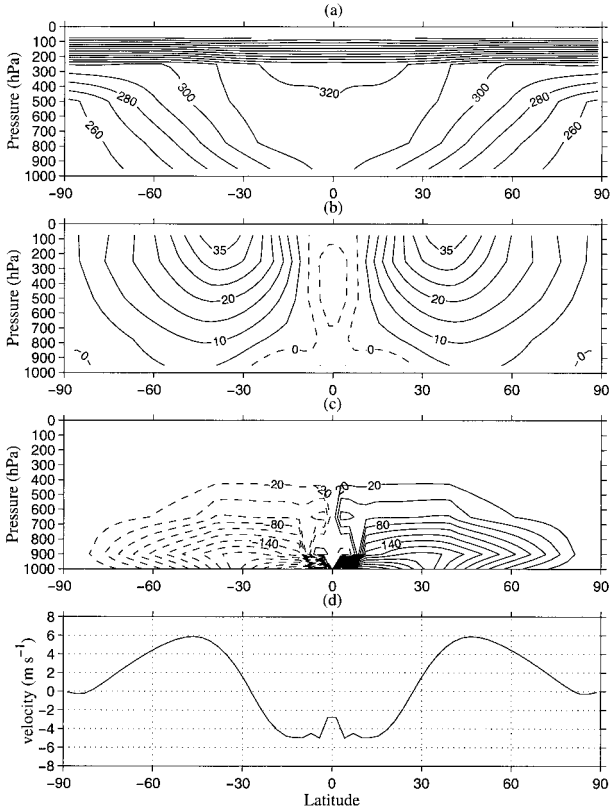

FIG. 21. The meridional cross sections after 1000 days for the experiment with parameterized PV fluxes, $\overline{v'q'} = 0$: (a) potential temperature, (b) zonal velocity, (c) residual mean overturning streamfunction, and (d) 950-mb winds.

integrated momentum flux is directed toward midlatitudes from the flanks of the westerly jets. The result is lateral momentum transfer that shifts the jet center northward from 25° to 38° latitude and generates midlatitude surface westerlies. The meridional profiles obtained in the parameterized model compare well to zonal-mean cross sections of the zonal wind component for observed annual conditions shown in Fig. 7.15a in Peixoto and Oort (1992). The only striking difference between the observed and modeled jets is the lack of distinct cores at height in the model. This is likely due to the low vertical resolution of the model at these levels.

3) EDDY FORCING: ZERO REYNOLDS STRESSES

We now neglect the relative vorticity fluxes in Eq. (5) as in the spindown of the baroclinic zone. Our scheme thus reduces to that of GM. The westerly jets in each hemisphere now have maxima at 25° latitude with values of 45 m s^{-1} (Fig. 23b). The meridional profile of potential temperature (Fig. 23a) is similar to that of the no eddy-forcing case. The residual overturning circulation extends toward the poles with a structure similar to that of the eddy-forced experiment, but some 60% weaker in magnitude. The meridional cross section of the eddy PV flux in the equilibrated state is plotted in Fig. 24a. It shows that, as before, there is a PV flux at the lower boundary with compensating convergence at mid heights in the troposphere. However the column-integrated eddy PV flux (Fig. 24b) is zero because relative vorticity fluxes have been ignored. There is no lateral momentum flux and only vertical transfer of momentum, which reduces the shear of the westerly jets and increases the low-level winds (see Fig. 23d). However, because of the neglect of lateral momentum fluxes, the eddy forcing of the mean flow is unable to change the position of the jet cores and sharpen the midlatitude westerlies.

It is well known that the tropospheric circulation cannot be modeled purely in terms of zonally symmetric processes; eddy buoyancy and momentum fluxes are crucial to the observed meridional structure and must be appropriately represented in order to achieve a realistic circulation. The three atmospheric experiments presented here clearly show that a realistic picture of the vertical and meridional distributions of mean zonal flow can only be attained when the full transfer characteristics of the eddies are represented.

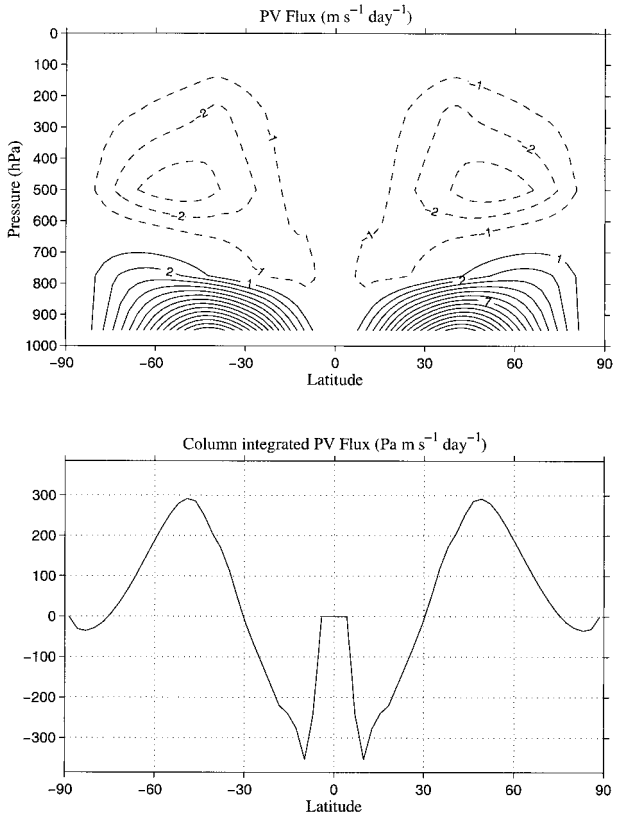

FIG. 22. (a) The eddy PV flux for the case shown in Fig. (7); (b) the column integrated PV flux. The eddies exert a westerly force at midlatitudes and easterly forces in the Tropics and toward the poles.

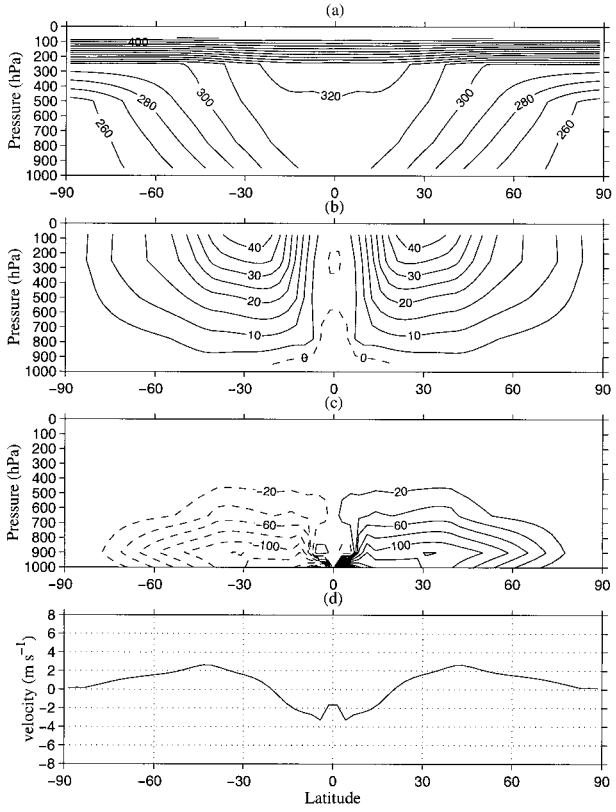

FIG. 23. The meridional profiles after 1000 days when Reynolds stress are set to zero in the parameterized model: (a) potential temperature, (b) zonal velocity, (c) residual mean overturning streamfunction, and (d) 950-mb winds.

7. Summary and conclusions

We have studied and attempted to parameterize the transfer properties of eddies in zonal channels by comparing eddy-resolved HPE models with their parameterized zonal-average counterparts. By focusing on potential vorticity, rather than separately on relative vorticity and thickness fluxes, the artificial separation between the transfer of heat and momentum (vorticity) is avoided and can be simultaneously captured. The theoretical context is not new, but by assuming that the eddies are quasigeostrophic while retaining full HPE form for the mean flow, we have been able to apply the formalism of the transformed Eulerian mean to a HPE model. This approach automatically leads to a representation in which advection is by the residual mean circulation. In the limit that eddy disturbances are quasigeostrophic the effect of the eddies appears as one term, an eddy PV flux driving the zonal momentum.

The eddy PV flux is assumed to be transferred down its mean gradient with a transfer coefficient K. The form of the K is chosen to ensure that an integral constraint on the eddy flux is satisfied so that the eddies act only to redistribute momentum in the flow. Downgradient PV flux does not, however, necessarily imply that momentum is diffused downgradient (e.g., $\overline{u'v'} = -k\overline{u}_y$). Indeed the approach can capture the sharpening of jets due to eddy–mean flow interaction on a β plane.

A limiting case of our approach leads to a different implementation of the scheme advocated by Gent and McWilliams (1990) in the zonal average. Their parameterization has led to improvements in water mass distributions and transport because they transform the buoyancy equation so that the eddy buoyancy flux terms become implicit. However, because the momentum equations are not also transformed, vorticity is arbitrarily transferred down its mean gradient. By using the complete TEM framework outlined here, we are able to encapsulate both the buoyancy and vorticity transporting properties of the eddy field, albeit in the zonal average, without having to parameterize them separately.

The theoretical arguments and eddy PV closure was tested using a three-dimensional, eddy-resolving, hydrostatic primitive equation model for stress-driven flow in a β-plane channel. The mean fields and eddy transfer characteristics of the eddy-resolving flow were compared to those of the same stress-driven flow in a parameterized model. The comparison shows that the transformed Eulerian mean approach offers advantages over existing parameterization schemes. The zonal mean fields of the parameterized model closely matched those

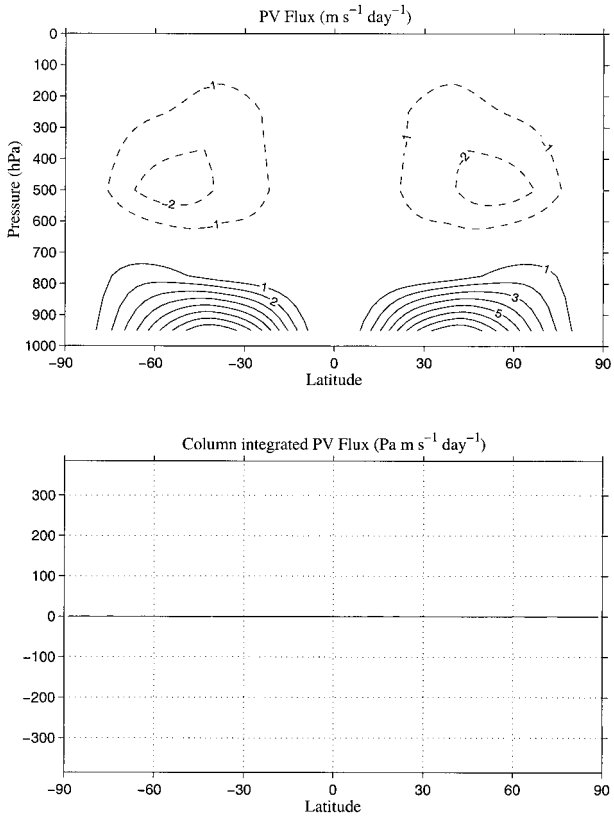

FIG. 24. The meridional cross sections of (a) the PV flux when Reynolds stresses are neglected, and (b) the column integrated PV flux. The column-integrated flux of PV is zero because relative vorticity fluxes have been ignored. There is no lateral momentum flux ($E^y = 0$) and so there is only vertical transfer of momentum associated with the lateral eddy buoyancy fluxes.

of the eddy resolving calculation in the equilibrated state. Study of two further flow configurations highlighted the advantages of representing eddies through a PV flux.

In a recent study Greatbatch (1998) advocates a parameterization scheme similar to the one above, based on the isopycnal, downgradient flux of PV. He notes that his scheme is not complete because parameterizing the eddy kinetic energy (EKE) terms in his time mean equation (89) is problematic. However, in the zonal mean, the EKE terms vanish in the zonal momentum equation and can be neglected in the meridional momentum equation if, as here, quasigeostrophic scaling for the eddies is assumed.

The approach to parameterization we advocate focuses, as have many others, on the eddy flux of potential vorticity rather than separately on thickness and relative vorticity fluxes. This strategy is not without its critics, however, because a simple relationship between PV flux and the large-scale gradient of PV is not always found. For example, Olbers et al. (2000) describes how potential vorticity mixing ideas need to be modified to understand eddy–mean flow interaction in a stress-driven, baroclinically unstable quasigeostrophic channel. But, although departures from $\overline{v'q'} = -\nabla\overline{q}$ are found, PV mixing driven by eddy enstrophy cascades is the canonical theoretical reference. Significantly Olbers et al. find no support for mixing of thickness with constant diffusivities in their numerical simulations. It should be noted, however, that Smith (1999) discusses the parameterization problem from a theoretical perspective and finds support for the idea of mixing of layer thickness from a stochastic theory of adiabatic stratified turbulence. This is achieved by making the Monin–Yaglom postulate, as first introduced in Dukowicz and Smith (1999). However, as a reviewer points out, Dukowicz and Greatbach (1999) avoid making this postulate and use an identity between the layer thickness flux and the PV flux that leads to support for PV mixing within the stochastic theory of turbulence. Nevertheless, the issue of layer thickness mixing needs to be further tested against eddy-resolved numerical experiments.

We have focused on problems that display a marked symmetry in the direction of the mean flow because it is the simplest context in which to proceed. With the zonally symmetric mean flows, the zonal symmetry displayed by the eddy statistics are implicit by design. This is due to there being no variation in the mean flow in the zonal direction. However, in the absence of a zonal-symmetric mean flow, advection of eddy PV variance by the mean flow give rise to a nonlocal contribution to the eddy fluxes, which may direct eddy transfer of PV upgradient. In spite of that, Marshall and Shutts (1981) show that for quasigeostrophic flows in which the mean PV is approximately conserved along mean streamlines the eddy PV flux can be separated into two parts: a rotational, nondivergent flux and an irrotational, divergent flux. The former balances the mean flow advection of the eddy PV variance and are associated with the spatial growth and decay of the eddies. The divergent flux balances the conversion from the mean field and is directed down the mean PV gradient if there is an enstrophy cascade. Thus a closure scheme based on downgradient transfer of PV may be appropriate, at least as a starting point, for gyrelike flows in which the zonal symmetry is broken.

We are studying whether the approach investigated here can be extended to three-dimensional flows and test if the divergent component of the eddy flux can be related to the mean gradient through transfer coefficients. This work is under way and will be reported in a later paper.

Acknowledgments. We would like to thank Alan Plumb for many helpful discussions that greatly clarified our understanding of the TEM formulation and the nature of quasigeostrophic eddies. Discussions with Alistair Adcroft and Chris Hill clarified numerical implementation issues. We are also grateful to the two anonymous reviewers for helping to greatly improve the manuscript.

Both RW and JM were supported by the NSF Physical Oceanography Program.

The numerical experiments reported here were carried out on an experimental computer called Pleiades, donated by Compaq/Digital and housed in the Laboratory for Computer Science at MIT.

APPENDIX

a. Calculation of the quasigeostrophic PV and its flux in a primitive equation model

The quasigeostrophic potential vorticity is computed in the primitive equation model using the definition

$$\overline{q}(y, z, t) = f_o + \beta y + \frac{\partial^2 \Psi}{\partial y^2} + f_o^2 \frac{\partial}{\partial z}\left(\frac{1}{N^2}\frac{\partial \Psi}{\partial z}\right), \quad \text{(A1)}$$

where

$$\psi = \frac{1}{\rho_o f_o}(p - p_o)$$

is the geostrophic streamfunction and $p_o(z)$ is the suitably defined horizontal mean reference pressure profile; $N^2 \equiv N^2(z) = \overline{b}_z^{xy}$ is the square of the horizontal mean buoyancy frequency. The geostrophic velocities are $(u, v) = (-\partial\psi/\partial y, \partial\psi/\partial x)$, and the buoyancy is given by $b = f_o \partial\psi/\partial z$.

In the limit of vanishing eddy relative vorticity fluxes, PV gradients are evaluated using

$$\overline{q}_{\text{stretching}}(y, z, t) = f_o^2 \frac{\partial}{\partial z}\left(\frac{1}{N^2}\frac{\partial \Psi}{\partial z}\right). \quad \text{(A2)}$$

The zonal mean meridional eddy flux of PV, $\overline{v'q'}$, is evaluated using the departures of v and q from the zonal average.

b. Upper and lower boundary conditions

1) ψ AND $\overline{Q}$

At the upper and lower boundaries the buoyancy distribution $b = f_o \partial\psi/\partial z$ provides inhomogeneous Neumann boundary conditions. A computational and conceptual simplification can be made if we replace the the inhomogeneous Neumann boundary conditions by homogeneous ones, following Bretherton (1966). This enables us to incorporate the boundary buoyancy distributions as parts of the interior PV distribution.

Let us define the quasigeostrophic potential vorticity $\tilde{q}(y, z)$, which is equal to $\overline{q}(y, z)$ in the fluid interior except adjacent to the horizontal boundaries. Just inside these boundaries, we place delta-function sheets of PV, δq_{upper} and δq_{lower}, of a strength and distribution chosen to represent the buoyancy variation on the boundary. Thus,

$$\tilde{q} = \overline{q} + \delta q_{\text{upper}} + \delta q_{\text{lower}}, \quad \text{(A3)}$$

where the delta-function sheets are given by

$$\delta q_{\text{upper}} = \frac{f_o^2}{N^2}\frac{\partial \overline{\psi}}{\partial z}\bigg|_{\text{upper}} \delta(z - z_{\text{upper}});$$

$$\delta q_{\text{lower}} = -\frac{f_o^2}{N^2}\frac{\partial \overline{\psi}}{\partial z}\bigg|_{\text{lower}} \delta(z - z_{\text{lower}}). \quad \text{(A4)}$$

In the numerical model these sheets manifest themselves in the top and bottom vertical levels of the model. The boundary conditions that go along with (3) are $\partial\psi/\partial z = 0$.

2) E AND $\overline{w}^*$

Because we choose to employ interior PV sheets together with the boundary condition $\partial\psi/\partial z = 0$, the buoyancy and lateral buoyancy flux at the horizontal boundaries necessarily vanishes. Hence the component of the Eliassen–Palm flux (E^z) through the boundary is zero, providing an integral constraint on momentum, Eq. (8). Moreover, from Eq (2b), this provides the needed boundary condition on the vertical component of the residual mean circulation at the upper and lower boundaries: $\overline{w}^* = 0$. The upper and lower boundary conditions on $\overline{w}^*$ are discussed in detail by Treguier et al. (1997). To avoid erroneously large $\overline{w}^*$ where isopycnals are vertical, they set the transfer coefficient for buoyancy to be zero at the upper and lower boundaries. This should be contrasted with the approach used here where PV transfer coefficients are nonzero adjacent to the boundary and act on PV gradients in the sheets.

REFERENCES

Andrews, D. G., and M. E. McIntyre, 1976: Planetary waves in horizontal and vertical shear: The generalized Eliassen–Palm relation and the mean zonal acceleration. *J. Atmos. Sci.,* **33,** 2031–2048.

——, J. R. Holton, and C. B. Leovy, 1987: *Middle Atmosphere Dynamics.* Academic Press, 489 pp.

Böning, C. W., W. R. Holland, F. O. Bryan, G. Danabasoglu, and J. C. McWilliams, 1995: An overlooked problem in model simulations of the thermohaline circulation and heat transport in the Atlantic Ocean. *J. Climate,* **8,** 515–523.

Bretherton, F., 1966: Critical layer instability in baroclinic flows. *Quart. J. Roy. Meteor. Soc.,* **92,** 325–334.

Brugge R., H. L. Jones, and J. C. Marshall, 1991: Non-hydrostatic ocean modeling for studies of open-ocean deep convection. *Deep Convection and Deep Water Formation in the Oceans,* P. C. Chu and J. C. Gascard, Eds., Elsevier Science, 325–340.

Danabasoglu, G., and J. C. McWilliams, 1995: Sensitivity of the global ocean circulation to parameterizations of mesoscale tracer transports. *J. Climate,* **8,** 2967–2978.

Dukowicz, J. K., and R. J. Greatbatch, 1999: The bolus velocity in the stochastic theory of ocean turbulent tracer transport. *J. Phys. Oceanogr.,* **29,** 2232–2239.

——, and R. D. Smith, 1999: Stochastic theory of compressible turbulent fluid transport. *Phys. Fluids,* **9,** 3523–3529.

Eliassen, A., and E. Palm, 1961: On the transfer of energy in stationary mountain waves. *Geofys. Publ.,* **22** (3), 1–23.

England, M., 1995: Using cloroflurocarbons to assess ocean climate models. *Geophys. Res. Lett.,* **22,** 3021–3054.

Gent, P. R., and J. C. McWilliams, 1990: Isopycnal mixing in ocean circulation models. *J. Phys. Oceanogr.,* **20,** 150–155.
——, and ——, 1996: Eliassen–Palm fluxes and the momentum equation in non-eddy resolving icean circulation models. *J. Phys. Oceanogr.,* **26,** 2539–2546.
——, J. Willebrand, T. J. McDougall, and J. C. McWilliams, 1995: Parameterizing eddy-induced tracer transports in ocean circulation models. *J. Phys. Oceanogr.,* **25,** 463–474.
Greatbatch, R. J., 1998: Exploring the relationship between eddy-induced transport velocity, vertical momentum transfer, and the isopycnal flux of potential vorticity. *J. Phys. Oceanogr.,* **28,** 422–432.
——, and K. G. Lamb, 1990: On parameterizing vertical mixing of momentum in non non-eddy-resolving models. *J. Phys. Oceanogr.,* **20,** 1634–1637.
Green, J., 1970: Transfer properties of the large-scale eddies and the general circulation of the atmosphere. *Quart. J. Roy. Meteor. Soc.,* **96,** 157–185.
Held, I. M., and A. Hou, 1980: Nonlinear axially symmetric circulations in a nearly inviscid atmosphere. *J. Atmos. Sci.,* **37,** 515–533.
——, and M. J. Suarez, 1994: A proposal for the intercomparison of the dynamical cores of atmospheric general circulation models. *Bull. Amer. Meteor. Soc.,* **75,** 1825–1830.
Hirst, A. C., and T. J. McDougall, 1998: Meridional overturning and dianeutral transport in a z-coordinate ocean model including eddy-induced advection. *J. Phys. Oceanogr.,* **28,** 1205–1223.
Jeffreys, H., 1926: On the dynamics of geostrophic winds. *Quart. J. Roy. Meteor. Soc.,* **52,** 85–102.
Johnson, G. C., and H. L. Bryden, 1989: On the size of the Antarctic Circumpolar Current. *Deep-Sea Res.,* **36,** 39–53.
Killworth, P. D., 1997: On the parameterization of eddy transfer. Part I: Theory. *J. Mar. Res.,* **55,** 1171–1197.
Lee, M. M., and H. Leach, 1996: Eliassen–Palm flux and eddy potential vorticity flux for a quasigeostrophic time-mean flow. *J. Phys. Oceanogr.,* **26,** 1304–1319.
Lorenz, E. N., 1967: The nature and theory of the general circulation of the atmosphere. WMO Publ. 218, World Meteorological Organization, Geneva, Switzerland, 161 pp.
Marshall, D. P., R. G. Williams, and M. M. Lee, 1999: On the relation between eddy-induced transport and the isopycnic gradients of potential vorticity. *J. Phys. Oceanogr.* **29,** 1571–1578.
Marshall, J., 1981: On the parameterization of geostrophic eddies in the ocean *J. Phys. Oceanogr.,* **11,** 257–271.
——, and G. Shutts, 1981: A note on rotational and divergent eddy fluxes. *J. Phys. Oceanogr.,* **11,** 1677–1680.
——, D. Olbers, H. Ross, and D. Wolf-Gladrow, 1993: Potential vorticity constraints on the dynamics and hydrography of the Southern Ocean. *J. Phys. Oceanogr.,* **23,** 465–487.
——, A. Adcroft, C. Hill, L. Perelman, and C. Heisey, 1997a: A finite volume, incompressible Navier Stokes model for studies of the ocean on parallel computers. *J. Geophys. Res.,* **102** (C3), 5753–5766.
——, C. Hill, L. Perelman, and A. Adcroft, 1997b: Hydrostatic, quasi-hydrostatic, and nonhydrostatic ocean modeling. *J. Geophys. Res.,* **102** (C3), 5733–5752.
McDougall, T. J., and P. C. McIntosh, 1996: The temporal-residual mean velocity. Part I: Derivation and the scalar conservation equations. *J. Phys. Oceanogr.,* **26,** 2653–2665.
McWilliams, J. C., W. R. Holland, and J. H. S. Chow, 1978: A description of numerical Antarctic Circumpolar currents. *Dyn. Atmos. Oceans,* **2,** 213–291.
Olbers, D., J. O. Wolff, and C. Völker, 2000: Eddy fluxes and second-order moment balances for nonhomogeneous quasigeostrophic turbulence in wind-driven zonal flows. *J. Phys. Oceanogr.,* **30,** 1645–1668.
Pavan, V., and I. M. Held, 1996: The diffusive approximation for eddy fluxes in baroclinically unstable jets. *J. Atmos. Sci.,* **53,** 1262–1272.
Peixoto, J. P., and A. H. Oort, 1992: *The Physics of Climate.* Springer-Verlag, 520 pp.
Plumb, R. A., and J. Mahlman, 1987: The zonally averaged transport characteristics of the GFDL general circulation/transport model. *J. Atmos. Sci.,* **44,** 298–327.
Rhines, P. B., 1977: The dynamics of unsteady currents. *The Sea,* E. Goldberg, Ed., Vol. 6, 189–318.
——, and W. B. Holland, 1979: Theoretical discussion of eddy-driven mean flows. *Dyn. Atmos. Oceans.,* **3,** 289–325.
——, and W. R. Young, 1982: Homogenization of potential vorticity in planetary gyres. *J. Fluid Mech.,* **122,** 347–367.
Robitaille, D. V., and A. J. Weaver, 1995: Validation of sub-grid scale mixing schemes using CFC's in a global ocean model. *Geophys. Res. Lett.,* **22,** 2917–2920.
Schubert, S., C. K. Park, W. Higgins, S. Moorthi, and M. Suarez, 1990: An atlas of ECMWF analyses (1980–1987). Part I—First moment quantities. NASA Tech. Memo. 100747.
Semtner, A. J., Jr., and R. M. Chervin, 1992: Ocean general circulation from a global eddy-resolving model. *J. Geophys. Res.,* **97** (C4), 5493–5550.
Smith, R., 1999: The primitive equations in the stochastic theory of adiabatic stratified turbulence. *J. Phys. Oceanogr.,* **29,** 1865–1880.
Starr, V. P., 1948: An essay on the general circulation of the earth's atmosphere. *J. Meteor.,* **5,** 39–43.
——, 1968: *The Physics of Negative Viscosity Phenomena.* McGraw-Hill, 256 pp.
Tandon, A., and C. Garret, 1996: On a recent parameterization of mesoscale eddies. *J. Phys. Oceanogr.,* **26,** 406–411.
Treguier, A. M., I. M. Held, and V. D. Larichev, 1997: Parameterization of quasigeostrophic eddies in primitive equation ocean models. *J. Phys. Oceanogr.,* **27,** 567–580.
Tung, K. K., 1986: Nongeostrophic theory of zonally averaged circulation. Part I: Formulation. *J. Atmos. Sci.,* **43,** 2600–2618.
Visbeck, M., J. Marshall, T. Haine, and M. Spall, 1997: On the specification of eddy transfer coefficients in coarse resolution ocean circulation models. *J. Phys. Oceanogr.,* **27,** 381–402.
Wiin-Nielsen, A., and J. Sela, 1971: On the transport of quasigeostrophic potential vorticity. *Mon. Wea. Rev.,* **99,** 447–468.